Mycobacterium tuberculosis Rv0991c is a redox-regulated molecular chaperone

Samuel H. Becker[1,2]*, Kathrin Ulrich[3], Avantika Dhabaria[4], Beatrix Ueberheide[4], William Beavers[5], Eric P. Skaar[5], Lakshminarayan M. Iyer[6], L. Aravind[6], Ursula Jakob[3] and K. Heran Darwin[1,]*

Running title: Redox-regulated chaperone

[1]Department of Microbiology, New York University School of Medicine, 430 E. 29th Street, Suite 312, New York, NY 10016, USA

[2]Current affiliation: Department of Microbiology and Immunology, University of Minnesota, 2101 6th Street SE, Campus Code 2641, Minneapolis, MN 55455

[3]Department of Molecular, Cellular, and Developmental Biology, University of Michigan, 1105 N. University Ave, Ann Arbor, MI 48109

[4]Proteomics Laboratory, Division of Advanced Research Technologies, New York University School of Medicine, 430 E. 29th Street, Suite 860, New York, NY 10016

[5]Vanderbilt Institute of Infection, Immunology, and Inflammation, Vanderbilt University Medical Center, Nashville, Tennessee, 37037

[6]National Center for Biotechnology Information, National Library of Medicine, National Institutes of Health, Bethesda, MD 20894, USA

*Address correspondence to samuelb51490@gmail.com or heran.darwin@med.nyu.edu

ABSTRACT

The bacterial pathogen *Mycobacterium (M.) tuberculosis* is the leading cause of death by an infectious disease among humans. Here, we describe a previously uncharacterized *M. tuberculosis* protein, Rv0991c, as a molecular chaperone that is activated by oxidation. Rv0991c has homologues in most bacterial lineages and appears to function analogously to the well-characterized *Escherichia coli* redox-regulated chaperone Hsp33, despite a dissimilar protein sequence. Rv0991c is transcriptionally co-regulated with *hsp60* and *hsp70* chaperone genes in *M. tuberculosis*, suggesting that Rv0991c functions with these chaperones in maintaining protein quality control. Supporting this hypothesis, we found that, like oxidized Hsp33, oxidized Rv0991c prevents the aggregation of a model unfolded protein *in vitro*, and promotes its refolding by the *M. tuberculosis* Hsp70 chaperone system. Furthermore, Rv0991c interacts with DnaK and associates with many other *M. tuberculosis* proteins. Importantly, we found Rv0991c is required for the full virulence of *M. tuberculosis* in mice. We therefore propose that Rv0991c, which we named "Ruc" (redox-regulated protein with unstructured C-terminus), represents a founding member of a new chaperone family that protects *M. tuberculosis* and other species from proteotoxicity during oxidative stress.

IMPORTANCE

M. tuberculosis infections are responsible for more than one million human deaths per year. Developing effective strategies to combat this disease requires a greater understanding of *M. tuberculosis* biology. As in all cells, protein quality control is essential for the viability of *M. tuberculosis*, which likely faces proteome stress within a host. Here, we identify an *M. tuberculosis* protein, Ruc, that gains chaperone activity upon oxidation. Ruc represents a previously unrecognized family of redox-regulated chaperones found throughout the bacterial super-kingdom. In addition to elucidating the activity of this chaperone, we found that Ruc was required for full *M. tuberculosis* virulence in mice. This work contributes to a growing appreciation that oxidative stress may provide a particular strain on protein stability in cells, and may likewise play a role in *M. tuberculosis* pathogenesis.

INTRODUCTION

The folding of a protein that is in a non-native conformation, including during translation or upon stress-induced denaturation, can be accomplished in all organisms by a set of chaperones belonging to the Hsp70 and Hsp40 protein families. In bacteria, these chaperones are called DnaK and DnaJ, respectively [reviewed in (1)]. DnaK is an ATPase that iteratively binds to and releases protein substrates, allowing them to fold into a native conformation. In the ATP-bound state, DnaK has high substrate affinity; substrate binding subsequently induces ATP hydrolysis in a DnaJ-dependent manner. The low-affinity, ADP-bound DnaK releases the client protein, which has either reached its native structure or can re-bind to DnaK (2, 3). This cycle of high- and low-affinity substrate-binding states is facilitated by a nucleotide exchange factor (NEF), which places the DnaK nucleotide-binding cleft in an open conformation; in bacteria, this activity is accomplished by a single DnaK-associated NEF, GrpE (4). Besides harboring intrinsic protein folding activity, the DnaK/DnaJ/GrpE system (DnaKJE) can also deliver substrates to GroEL/GroES chaperonins (also known as Hsp60/Hsp10), and eukaryotic DnaKJE homologs can cooperate with proteases to promote the degradation of unfolded substrates (5-7).

Proteins in non-native conformations often expose hydrophobic regions that are prone to aggregation, an event that is toxic to cells. Importantly, aggregate formation becomes irreversible if DnaKJE cannot access unfolded proteins for refolding. To remedy this situation, the Hsp100 family of ATP-dependent chaperones (called ClpB in bacteria) cooperate with DnaKJE by solubilizing proteins within aggregates (8-10). The prevention of irreversible protein aggregation is also accomplished in all organisms by the small heat shock protein (sHsp) family of chaperones. Rather than actively dissociating protein

aggregates by ATP hydrolysis, sHsps act by simply binding to denatured or misfolded proteins; the presence of sHsps within protein aggregates allows for efficient refolding by ATPase chaperones (5, 11-14). Thus, in contrast to “refoldases”, sHsps are “holdases” that afford cells the ability to rapidly respond to proteotoxic stress in an energy-independent manner.

While DnaKJE, chaperonins, ClpB, and sHsps are all active under steady-state conditions, there are also non-canonical chaperones that only become active upon encountering specific stresses. Hsp33 (encoded by *hslO*), found in both prokaryotes and eukaryotes, and the eukaryotic Get3 are inactive as chaperones in the normal reducing environment of the cytoplasm; however, oxidation of cysteine thiols within Hsp33 or Get3 induces conformational changes that allow them to bind to unfolded proteins (6, 15-18). Hsp33 prevents the irreversible aggregation of unfolded proteins by delivering substrates to ATPase chaperones for refolding (6). In *E. coli*, this activity is of particular importance during heat and oxidative stress, during which low ATP levels cause DnaK to enter a partially unfolded, nucleotide-depleted state; the presence of Hsp33 allows for refolding by DnaKJE to proceed once a normal temperature and reducing environment is restored (19). Another bacterial chaperone, RidA, is activated by the oxidant hypochlorous acid through a mechanism that does not involve oxidation of cysteine thiols, but rather chlorination of its free amino groups (20). Aside from oxidation, other non-canonical chaperones have been found to activate upon exposure to high temperatures or acid [reviewed in (21)].

The bacterial pathogen *M. tuberculosis* is currently responsible for the majority of human infectious disease-related deaths worldwide (22). In this work, we describe our

discovery that the uncharacterized *M. tuberculosis* gene Rv0991c encodes a chaperone, which we named Ruc (redox-regulated chaperone with unstructured C-terminus). Ruc belongs to a previously unacknowledged, but evolutionarily widespread family of bacterial proteins with little predicted structural similarity to other chaperones. Upon oxidation, Ruc is capable of inhibiting protein aggregation and delivering unfolded proteins to DnaKJE for refolding. Ruc was also found to interact with DnaK in *M. tuberculosis* and, while dispensable for *in vitro* growth, was required for full *M. tuberculosis* virulence in mice. These observations ultimately suggest that Ruc is important for the ability of *M. tuberculosis*, and potentially many other bacterial species, to withstand oxidation-associated proteotoxicity.

RESULTS

Ruc induction during heat stress requires the *M. tuberculosis* Pup-proteasome system. We became interested in Ruc after identifying the transcriptional repressor HrcA as a putative target of the *M. tuberculosis* Pup-proteasome system (23). In *M. tuberculosis*, HrcA directly represses four genes; three of them encode highly conserved chaperone proteins of the Hsp60/Hsp10 family, while the fourth gene, *ruc*, encodes a protein of unknown function (24). In addition to its negative regulation by HrcA, *ruc* is induced during heat stress by SigH, a sigma factor that also activates transcription of the Hsp70/Hsp40 genes (25). The DNA sequences to which SigH and HrcA bind upstream of the *ruc* start codon overlap, suggesting that these two transcriptional regulators compete for binding to the *ruc* promoter (**Fig. 1A**). We compared Ruc abundance upon incubation of *M. tuberculosis* at 37ºC or 45ºC and found that Ruc levels increased

dramatically at 45ºC, consistent with previously reported transcriptional data (**Fig. 1B, lanes 1 and 2**) (24). The low abundance of Ruc at 37ºC is primarily due to repression by HrcA, given that Ruc was highly abundant in an *hrcA* mutant at this temperature (**Fig. 1B, lane 5**). We observed a further induction of Ruc levels during heat shock in an *hrcA* mutant (**Fig. 1B, lane 6**). These results corroborate earlier evidence that *ruc* expression is controlled in two ways: through repression by HrcA and induction by SigH.

In a recent study, we proposed that the pupylation and degradation of HrcA by the *M. tuberculosis* proteasome is required for the full expression of the HrcA regulon. We previously reported the abundance of HrcA-regulated gene products between a wild type (WT) *M. tuberculosis* strain and an *mpa* mutant, which cannot degrade pupylated proteins, and found that GroES, GroEL1, and GroEL2 levels are significantly lower in an *mpa* strain; however, Ruc abundance is unaffected by disruption of *mpa* under these conditions. This result suggested that proteasomal degradation of HrcA is not sufficient for Ruc production under the conditions tested (23); however, this experiment was performed with cultures incubated at 37ºC in minimal medium. We therefore compared Ruc abundance from the same strains incubated at 45ºC and observed a striking defect in Ruc production in the *mpa* mutant (**Fig. 1C, lane 2**). This result supports the hypothesis that the proteasomal degradation of HrcA is required for *M. tuberculosis* to robustly induce *ruc* expression during heat stress.

Ruc is required for the full virulence of *M. tuberculosis*. Previous studies have shown that *M. tuberculosis* protein quality control pathways are important for its pathogenesis. *M. tuberculosis* strains deficient in *clpB* or the sHsp-encoding *acr2* have impaired

143 virulence in mice (26, 27), while a mutant lacking HspR, which represses the expression
144 of *clpB*, *acr2*, and the *hsp70/hsp40* genes, also produces less severe infections (28).
145 Because *ruc* is co-regulated with essential chaperones, we tested if Ruc were required
146 for the full virulence of *M. tuberculosis*. We inoculated mice with *M. tuberculosis* strains
147 by aerosol, and assessed bacterial burden in the lungs and spleen at several time points
148 following infection. At three- or eight- weeks post-infection, a *ruc* mutant did not display a
149 significant survival defect compared to a WT strain. However, after 27 weeks, we
150 recovered approximately five-fold fewer bacteria from the lungs of mice infected with the
151 *ruc* mutant than from those infected with WT or *ruc* complemented strains (**Figure 1D,**
152 **top panel**). Bacterial burden in the spleen was not significantly different between
153 infections at any time point (**Figure 1D, bottom panel**). While the virulence phenotype of
154 the *ruc* mutant was modest, our results indicate that Ruc may be important for *M.*
155 *tuberculosis* survival in the lungs during the chronic stage of an infection.
156
157 **Ruc is part of a novel protein family found across the bacterial super-kingdom.**
158 According to the mycobacterial genome database MycoBrowser, Ruc is conserved in
159 both pathogenic and non-pathogenic mycobacteria (29). To determine the broader
160 phyletic distribution of Ruc among bacteria, we searched the Ruc protein sequence
161 against a curated collection of 7,423 complete prokaryotic genomes. Ruc is highly
162 conserved throughout the planctomycetes, chloroflexi, delta- and beta- proteobacteria,
163 actinobacteria, spirochaetes, and verrucomicrobiae lineages; additionally, Ruc is found
164 in species within other major bacterial lineages such as gammaproteobacteria, firmicutes

and cyanobacteria. This phyletic pattern suggests that Ruc was present in the last bacterial common ancestor, with rare lateral transfers to archaea (**Table 2**).

To define the conserved features of Ruc, we used Phyre2, a program that predicts secondary and tertiary protein structures based on published sequences and solved structures (30). Alignment of Ruc with its homologs in other bacteria identified two conserved domains. The amino (N)-terminal region, consisting of approximately 50 amino acids, contains four cysteine (Cys) residues arranged in a manner consistent with a zinc ribbon fold, a domain found in zinc-binding proteins of highly diverse functions (**Fig. 2A**) (31). The carboxyl (C)-terminal regions of Ruc homologs consist of highly variable sequences of amino acids ranging in length from approximately seven to 61 residues. While these C-terminal domains do not share significant similarity at the protein sequence level, they appear to be uniformly composed of hydrophilic residues with no predicted secondary structure. Overall, these structural predictions allowed us to conclude that *M. tuberculosis* Ruc and its homologs are likely characterized by a metal-coordinating N-terminal domain and a disordered C-terminus (**Fig. 2B**).

Having established that *ruc* is co-expressed with the Hsp60 and Hsp70 chaperone system genes in *M. tuberculosis* and is present in diverse bacterial lineages, we next asked if *ruc* is associated with protein quality control genes in other species. A comprehensive gene neighborhood analysis among bacteria recovered widespread associations with chaperone genes, as well as transcription factors and proteases that regulate chaperone production. In bacteria of the PVC (Plantomycetes, Verrucomicrobia, Chlamydiae) and FCB (Fibrobacteres, Chlorobi, Bacteroidetes) superphyla, *ruc* is present in loci encoding DnaK, DnaJ, GrpE, ClpB, alpha-crystallin sHsps (Acr), and HrcA. In

bacteria from the Chloroflexi phylum, as well as several unclassified species, Ruc is additionally associated with GroES/GroEL chaperonins, the chaperone-regulating protease FtsH, and the redox-regulated chaperone RidA (**Fig. 2C**). The identification of these conserved genetic linkages, as well as the observation that *ruc* is transcriptionally co-regulated with essential chaperone genes in *M. tuberculosis*, allowed us to conclude that Ruc most likely performs a function related to protein folding.

Ruc coordinates zinc and is an intrinsically disordered protein. Based on the observations that *ruc* is closely associated with essential chaperone genes and that Ruc contains putative zinc-coordinating cysteines, we hypothesized that Ruc has oxidation-dependent chaperone activity. Hsp33 and Get3, the only chaperones currently described whose activity requires cysteine oxidation, each contain a zinc-coordinating domain consisting of four cysteines. Under oxidizing conditions, these cysteines form intramolecular disulfide bonds and release zinc, allowing these chaperones to form complexes with denatured proteins to prevent their irreversible aggregation (15, 17, 32).

To begin to test Ruc chaperone activity using *in vitro* assays, we produced and purified *M. tuberculosis* Ruc from *E. coli* under reducing conditions (Ruc_{red}). We oxidized purified Ruc (Ruc_{ox}) by incubation with hydrogen peroxide (H_2O_2) and copper chloride ($CuCl_2$), which react to generate hydroxyl radicals that rapidly oxidize cysteines (33). On an SDS-PAGE gel, Ruc_{red} migrated as a single band (**Fig. 3A, lane 1**) while Ruc_{ox} migrated through the gel as multiple species, whose sizes were consistent with the formation of covalent, intermolecular disulfide bonds (**Fig. 3A, lane 2**). Treatment of Ruc_{ox} with the thiol-reducing agent dithiothreitol (DTT) resulted in a significant loss of higher-

molecular weight species, indicating that the oxidation of Ruc cysteines is reversible (**Fig. 3A, lane 3**). These results demonstrate that Ruc cysteines form disulfide bonds under oxidizing conditions to create covalently-linked multimers.

In Hsp33, four conserved cysteines coordinate zinc. This zinc binding maintains Hsp33 in an inactive state, yet allows Hsp33 to become readily activated once an oxidant is present (32). To determine if Ruc binds zinc using its four cysteines, we used 4-(2-pyridylazo)resorcinol (PAR), a chemical that chelates free zinc to yield an absorbance peak at 500 nm (A_{500}) (see Materials and Methods). Incubation of either Ruc_{red} or Ruc_{ox} with PAR alone did not yield a significant change in A_{500}, demonstrating that the protein preparations contained little free zinc; however, addition of N-ethylmaleimide (NEM), which forms adducts on cysteine thiols, resulted in the release of zinc from Ruc_{red} that could be detected in approximately equimolar abundance to Ruc_{red}. Meanwhile, addition of NEM to Ruc_{ox} did not reveal any change in zinc levels (**Fig. 3B**). These data suggest that under reducing conditions, Ruc cysteines coordinate an atom of zinc, and that this binding is disrupted when the cysteine thiols are oxidized.

Given that PAR can chelate metals in addition to zinc (34), we next determined the precise identity of the metal bound to Ruc using inductively coupled plasma mass spectrometry (ICP-MS). In this analysis, we found zinc was present in Ruc_{red} preparations in close to equimolar amounts; when Ruc_{red} was treated with NEM prior to ICP-MS, little Ruc-bound zinc was detected (**Table S1**). Taken together, our metal-binding assays demonstrated that cysteine thiols in Ruc coordinate a single zinc atom.

Aside from the N-terminal zinc ribbon fold domain, the entire C-terminal half of Ruc was predicted to lack secondary structure (**Fig. 2B**). To evaluate the degree of disorder

234 in Ruc, we measured the secondary structures found in Ruc_{red} and Ruc_{ox} using circular
235 dichroism (CD) spectroscopy [reviewed in (35)]. In accordance with structural predictions,
236 both Ruc_{red} and Ruc_{ox} yielded a CD spectrum characteristic of disordered proteins (**Fig.**
237 **3C**) (36). The high degree of disorder present in Ruc, along with our previous observation
238 that all Ruc homologs are predicted to harbor domains that lack secondary structure,
239 support a hypothesis whereby the unstructured C-terminal domain somehow contributes
240 to the function of this protein.
241
242 **Oxidized Ruc prevents unfolded protein aggregation *in vitro*.** Chaperones are able
243 to inhibit protein aggregation due to their propensity to bind to unfolded proteins. A
244 common method for detecting chaperone activity uses purified firefly luciferase, which
245 denatures and forms irreversible aggregates when heated above 42ºC; the presence of
246 a chaperone during denaturation of luciferase prevents its aggregation (15, 37). We
247 therefore used this method to test chaperone activity by Ruc. When we incubated
248 luciferase at 45ºC, we observed the formation of precipitates that could be detected by
249 an increase in light absorbance at 350 nm. In the presence of a fivefold molar excess of
250 Ruc_{red}, we observed a similar level of luciferase aggregation, demonstrating that Ruc_{red}
251 has little to no chaperone activity. In contrast, the presence of Ruc_{ox} during heat
252 inactivation, either in excess or at an equimolar concentration, significantly inhibited
253 luciferase aggregation (**Fig. 4A**). When we measured luciferase aggregation using a
254 different method of detection, dynamic light scattering (38), we also observed the
255 inhibition of aggregation by Ruc_{ox}, but not by Ruc_{red} (**Fig. S1A**). Furthermore, chaperone
256 activity by Ruc was observed when Ruc was pre-treated with the oxidizing agents

hypochlorite or nitric oxide (**Fig. S1B**), further supporting a model whereby oxidized Ruc counteracts protein aggregation.

In the activation process of Hsp33, oxidation induces conformational changes that expose a disordered region with high affinity for client proteins (39, 40). We therefore asked if the intrinsically disordered C-terminal domain of Ruc was required for its chaperone activity. We produced a truncated Ruc variant, Ruc_{Nterm} (amino acids 1 through 49), which harbors only the zinc binding motif (**Fig. 4B, lane 2**). Oxidized Ruc_{Nterm} ($Ruc_{Nterm\text{-}ox}$) formed a single high-molecular weight species, in contrast to the variety of multimers observed for Ruc_{ox} (**Fig. 4B, lanes 3 and 4**). When we tested the chaperone activity of oxidized Ruc_{Nterm} ($Ruc_{Nterm\text{-}ox}$), we found that it was unable to prevent luciferase aggregation (**Fig. 4C**). Thus, the disordered C-terminus of Ruc is required for its chaperone activity, either by binding to client protein, by influencing the conformation or oligomerization state of Ruc, or through a combination of factors.

We next asked if replacing the Ruc cysteines, which we predicted would disrupt zinc coordination, would allow for constitutive Ruc activity in the absence of oxidation, a phenomenon that was observed for Hsp33 (32). We made cysteine (C) to serine (S) substitutions in Ruc, generating $Ruc_{C8S,C11S}$ and $Ruc_{C29S,C32S}$ (see Table 1 for primers and plasmids). Neither $Ruc_{C8S,C11S\text{-}red}$ nor $Ruc_{C29S,C32S\text{-}red}$ were bound to zinc upon their purification (**Fig. 4D**). When we tested the ability of each reduced Ruc variant to inhibit luciferase aggregation, we found that both exhibited significant chaperone activity compared to wild-type Ruc_{red} (**Fig. 4E**). Collectively, these results support a model by which Ruc is in a zinc-bound, inactive state under reducing conditions, and that oxidation

and zinc release promotes a conformation of Ruc that allows for its interaction with an unfolded protein.

Oxidized Ruc promotes protein refolding by *M. tuberculosis* Hsp70/Hsp40 chaperones. Non-ATPase bacterial chaperones such as Hsp33 and sHsps prevent irreversible protein aggregation *in vivo*; critically, this function relies on the ability of ATP-dependent chaperones to eventually refold substrates that are bound by these non-ATPase chaperones (5, 6, 41). To further understand the potential role of Ruc in *M. tuberculosis* protein quality control, we tested if Ruc could promote protein refolding by *M. tuberculosis* DnaKJE. To test this hypothesis, we heated luciferase either alone or in the presence of Ruc_{red} or Ruc_{ox}; after bringing the reaction to room temperature and adding purified *M. tuberculosis* DnaK, DnaJ2, and GrpE under reducing conditions, we monitored refolding by measuring luciferase activity over time. Only minimal refolding of luciferase by DnaKJE was observed when luciferase was denatured in the absence of a chaperone, a result that was expected based on previous studies (5, 6, 11, 41). By contrast, significant DnaKJE-mediated refolding of luciferase was achieved when luciferase was denatured in the presence of Ruc_{ox} (**Fig. 5A**). Consistent with its inability to prevent luciferase aggregation (**Fig. 4A**), Ruc_{red} had no significant effect on luciferase refolding (**Fig. 5A**). These results demonstrate that unfolded proteins that are bound by Ruc under oxidizing conditions can be delivered to the DnaKJE system for refolding.

After establishing the chaperone activity of Ruc *in vitro*, we sought to better understand the specific role of Ruc in *M. tuberculosis* physiology by identifying potential protein interaction partners *in vivo*. To capture such interactions, we produced Ruc with

a hexahistidine-FLAG tandem affinity purification tag (Ruc_{TAP}) in *M. tuberculosis*. When we performed a two-step purification of Ruc_{TAP} from *M. tuberculosis* lysates under native conditions, we observed that a second protein co-purified with Ruc_{TAP} (**Fig. 5B**); mass spectrometry identified this protein as DnaK (see Materials and Methods). We validated the identity of DnaK in Ruc_{TAP} purifications by immunoblotting with a monoclonal antibody to DnaK (**Fig. S2A**). Importantly, this result was specific to Ruc_{TAP}, as DnaK did not co-purify with another small TAP-tagged protein, $PrcB_{TAP}$ (**Fig. S2A**). This apparent interaction between Ruc and DnaK in *M. tuberculosis* lysates supports the hypothesis that Ruc is directly involved in maintaining protein folding by the DnaKJE system *in vivo*.

Notably, Ruc_{TAP} interacted with DnaK under native purification conditions in which no oxidants were added. Given that Ruc chaperone function is activated under oxidizing conditions, we next sought to capture the interaction of Ruc with endogenous client proteins by purifying Ruc_{TAP} from bacteria subjected to oxidative stress, a condition that could promote association of Ruc_{TAP} with unfolded substrates. However, when we purified Ruc_{TAP} from *M. tuberculosis* cultures that were exposed to a sub-lethal concentration of H_2O_2 and $CuCl_2$ at 45ºC, we did not observe any additional proteins co-purifying with Ruc_{TAP} (**Fig. S2B**). We hypothesized that intact *M. tuberculosis* rapidly reverses oxidation, such that interactions between Ruc_{ox} and unfolded client proteins are too transient to capture. We instead treated lysates of Ruc_{TAP}-producing *M. tuberculosis* with H_2O_2 and $CuCl_2$, and found that oxidation resulted in the association of many *M. tuberculosis* proteins with Ruc_{TAP} (**Fig. 5C, lane 2**). To determine the identity of these putative clients of Ruc, we performed proteomic mass spectrometry to identify the proteins that co-purified with Ruc_{TAP} under oxidizing, but not native conditions (**Table S2**). Proteins that

co-purified with activated Ruc$_{TAP}$ were associated with a diverse range of functions including nitrogen and carbon metabolism, electron transport, oxidative stress, and transcriptional regulation; thus, Ruc chaperone activity likely provides a general protective effect on the *M. tuberculosis* proteome during oxidation. Importantly, while these results suggest that Ruc can interact with a wide variety of proteins, we are currently unable to verify that the same interactions take place within bacteria under the same conditions.

Ruc is not essential for *M. tuberculosis* resistance to oxidation. During an infection, *M. tuberculosis* primarily resides within macrophages. These and other immune cells are capable of mounting an antimicrobial response that includes the generation of reactive oxygen species (ROS), reactive nitrogen intermediates (RNI), and hypochlorite. These molecules, all of which can react with cysteine thiols, can confer lethal stress upon infecting pathogens [reviewed in (42)]. Animals defective in the ability to produce ROS, RNI, and hypochlorite are more susceptible to bacterial and fungal pathogens (43-46), and human deficiency in ROS production is associated with susceptibility to mycobacterial infections (47).

Our data thus far led us to hypothesize that Ruc contributes to *M. tuberculosis* virulence by protecting bacteria from protein aggregation during oxidative stress. Therefore, we sought to test if a *ruc* mutant was more susceptible to a variety of oxidative stress conditions *in vitro*. We challenged *M. tuberculosis* strains incubated at 45ºC with either peroxide, hypochlorite, plumbagin (which generates superoxide radicals in cells) (48), or acidified nitrite (which produces NO) (49) and measured the approximate lethal dose of each compound. Interestingly, the WT and *ruc* mutant strains were equally

susceptible to killing under all stress conditions tested (**Fig. S3**). Thus, despite the observation that the *ruc* mutant has a subtle virulence defect in mice, we were unable to conclusively determine if Ruc protects *M. tuberculosis* from the various oxidative stress conditions that might be encountered in a host. Given that *M. tuberculosis* has multiple mechanisms for maintaining bacterial redox balance, including thioredoxins, mycothiol and catalase [reviewed in (50)], it is possible that the contribution of Ruc to *M. tuberculosis* fitness only becomes apparent under conditions in which these antioxidant systems are not fully effective; notably, the requirement for Hsp33 for *E. coli* resistance to oxidative stress is observed only after the thioredoxin system is genetically disrupted (16).

DISCUSSION

In this study, we identified Ruc as the founding member of a new family of bacterial redox-regulated chaperones. Prior to this work, Hsp33 and RidA were the only other proteins described in bacteria whose chaperone activity is dependent on oxidation. Remarkably, however, Ruc shares no sequence similarity to these proteins aside from the presence of four zinc-coordinating cysteines, a feature of Hsp33. Reduced, inactive Hsp33 compactly folds into two globular domains; a combination of high temperature and oxidation causes partial unfolding of the protein, exposing a disordered region with high affinity for substrates (39, 40). The Hsp33 zinc-binding motif, while essential for inducing conformational changes upon oxidation, does not directly participate in substrate binding (39). In contrast to Hsp33, Ruc likely has a single, small globular region, and is predicted to be intrinsically disordered across more than half the length of the protein. We therefore expect that the mechanism of its activation is distinct from that of Hsp33. Our observation

371 that Ruc$_{red}$ has no chaperone activity could suggest that the disordered domain of Ruc$_{red}$
372 is kept in a partially occluded state, perhaps by interacting with other regions of the
373 protein, and would therefore be unavailable for binding a client protein until oxidation
374 takes place. Structural studies of Ruc, both alone and in complex with a substrate, will be
375 necessary to determine the precise mechanism of its activation.

376 It is well-established that Hsp33 and sHsps deliver unfolded proteins to ATPase
377 chaperones for refolding (5, 6, 41). Here, we describe a similar function of Ruc in
378 promoting protein folding by *M. tuberculosis* DnaKJE (**Fig. 6**). Importantly, despite strong
379 evidence that proteins can be directly transferred from non-ATPase to ATPase
380 chaperones, a direct interaction between a holdase and a foldase has never been
381 observed (14). Thus, our ability to capture the interaction of Ruc and DnaK, even in the
382 absence of an environmental stress, may present a new opportunity to understand
383 mechanisms by which holdases transfer their substrates to DnaK.

384 Supporting the hypothesis that Ruc contributes to *M. tuberculosis* pathogenesis,
385 a previous screen to identify genes required for *M. tuberculosis* virulence in mice found
386 that bacteria with transposon insertions in *ruc* are defective for *in vivo* growth during mixed
387 infections (51). In another study, mice infected with an *M. tuberculosis* strain containing
388 a deletion-disruption of Rv0990c (encoding Hsp22.5), the gene directly downstream of
389 *ruc*, had a lower bacterial burden during the later stages of infection and increased time
390 to death compared to mice infected with a WT strain; however, the phenotypes in this
391 study could not be fully complemented (52). Conceivably, the Rv0990c mutation could
392 have affected Ruc production, which might explain the incomplete complementation of
393 the Rv0990c mutation to fully restore virulence.

394 The widespread conservation of Ruc homologues suggests that this protein
395 protects bacteria against one or more common environmental stresses, and not just host-
396 exclusive factors. Notably, with the exception of a single species, Hsp33 homologs are
397 absent from the Actinobacteria; by contrast, Ruc homologs are found throughout this
398 phylum, including the majority of mycobacterial species [STRING database (53)]. We
399 therefore speculate that for these species, Ruc fulfills a similar role to that of Hsp33:
400 preventing the irreversible aggregation of unfolded proteins during oxidative stress, a
401 condition in which ATP depletion or direct thiol modification of DnaK may render DnaKJE-
402 mediated refolding impossible (6, 19, 54). If this scenario were indeed supported by
403 further studies, then Ruc and Hsp33, which appear to be structurally unrelated, may
404 represent products of convergent evolution.
405
406 **Materials and Methods**
407 **Strains, plasmids, primers, and culture conditions**. See Table 1 for strains, plasmids,
408 and primers used in this work. Reagents used for making all buffers and bacterial media
409 were purchased from Thermo Fisher Scientific, unless otherwise indicated. *M.*
410 *tuberculosis* was grown in "7H9c" [BD Difco Middlebrook 7H9 broth with 0.2% glycerol
411 and supplemented with 0.5% bovine serum albumin (BSA), 0.2% dextrose, 0.085%
412 sodium chloride, and 0.05% Tween-80]. For the experiment in Figure 1C, bacteria were
413 grown in Proskauer-Beck minimal medium supplemented with asparagine and a similar
414 result was observed in 7H9c. For solid media, *M. tuberculosis* was grown on "7H11" agar
415 (BD Difco Middlebrook 7H11) containing 0.5% glycerol and supplemented with 10% final
416 volume of BBL Middlebrook OADC Enrichment. For selection of *M. tuberculosis*, the

following antibiotics were used as needed: kanamycin 50 µg/ml, hygromycin 50 µg/ml. *E. coli* was cultured in BD Difco Luria-Bertani (LB) broth or on LB Agar. Media were supplemented with the following antibiotics as needed: kanamycin 100 µg/ml, hygromycin 150 µg/ml, ampicillin 200 µg/ml.

Primers used for PCR amplification or sequencing were purchased from Life Technologies and are listed in Table 1. DNA was PCR-amplified using either Phusion (New England Biolabs; NEB), Pfu (Agilent), or Taq (Qiagen) according to the manufacturers' instructions. PCR products were purified using the QIAquick Gel Extraction Kit (Qiagen). Plasmids encoding His_6-SUMO-Ruc, His_6-SUMO-Ruc_{Nterm}, His_6-SUMO-$Ruc_{C8S,C11S}$ and His_6-SUMO-$Ruc_{C29S,C32S}$ were made using splicing by overlap extension (SOE) PCR (55). Restriction enzymes and T4 DNA ligase were purchased from NEB. The following plasmids were made by PCR-amplifying genes from *M. tuberculosis* DNA using the indicated primers and cloning amplification products into their respective vectors: pET24b(+)-Rv0991c-his_6 (NdeI-Rv0991c-F, HindIII-Rv0991c-R), pMV306kan-Rv0991c (HindIII-Rv0991c-F, XbaI-Rv0991c-R), pOLYG-Rv0991c-TAP (HindIII-Rv0991c-F, XbaI-Rv0991c-TAP-R), pAJD107-Rv0991c (NdeI-Rv0991c-F, BglII-Rv0991c-R), pAJD107-Rv0991c-C8S,C11S (NdeI-Rv0991c-C8S,C11S-F, BglII-Rv0991c-R). pET24b(+)-Rv0991c and pET24b(+)-Rv0991c-C8S,C11S were made by subcloning the Rv0991c gene from pAJD107-Rv0991c and pAJD107-Rv0991c-C8S,C11S into pET24b(+), respectively. pET24b(+)-HisSUMO-*ruc* was made by first PCR-amplifying HisSUMO from pEcTL02 using primers T7-F and SUMO-Ruc-soeR, secondly amplifying *ruc* from *M. tuberculosis* DNA using SUMO-Ruc-soeF and Ruc-KpnI-R, and finally performing SOE PCR using these two amplification products along with

primers T7-F and Ruc-Kpn-R. The SOE PCR product was then cloned into pET24b(+). pET24b(+)-HisSUMO-*ruc*-Nterm was made similarly, except that the primer RucNterm-KpnI-R substituted for Ruc-KpnI. pET24b(+)-HisSUMO-*ruc*-C29S,C32S was made by SOE PCR using primers T7-F, T7-term, Rv0991c-C29SC32S-F and Rv0991c-C29SC32S-R, with pET24b(+)-HisSUMO-*ruc* as the PCR template. pET24b(+)-HisSUMO-*ruc*-C8SC11S was made similarly to pET-24b(+)-HisSUMO-*ruc*, except that the amplification product from primers SUMO-Ruc-soeF and Ruc-KpnI-R was made using pET24b(+)-Rv0991c-C8S,C11S as a template.

Calcium chloride-competent *E. coli* DH5α was transformed with ligations. All plasmids were purified from *E. coli using* the QIAprep Spin Miniprep Kit. All plasmids made by PCR cloning were sequenced by GENEWIZ, Inc. to ensure the veracity of the cloned sequence. Plasmids were transformed into *M. tuberculosis* by electroporation as previously described (56). Single-colony transformants were isolated on 7H11 agar with antibiotic selection.

Protein purification, antibody production, and immunoblotting. Ruc-His_6 was produced in *E. coli* strain ER2566; His_6-SUMO-Ruc, His_6-SUMO-RucNterm, His_6-SUMO-$Ruc^{C8S,C11S}$, His_6-SUMO-$Ruc^{C29S,C32S}$, His_6-SUMO-DnaK, His_6-SUMO-DnaJ2, His_6-SUMO-GrpE, and His_6-Ulp1 were produced in *E. coli* strain BL21. Proteins were purified from *E. coli* by affinity chromatography using Ni-NTA agarose (Qiagen) according to the manufacturer's instructions (Ruc-His_6 was purified under urea denaturing conditions). Production of His_6-SUMO-DnaK, His_6-SUMO-DnaJ2, and His_6-SUMO-GrpE in *E. coli* was

462 performed as previously described (11). To make rabbit polyclonal immune serum,
463 approximately 200 µg Ruc-His_6 was used to immunize rabbits (Covance, Denver, PA).
464 *M. tuberculosis* Ruc was prepared from *E. coli* using two methods that yielded
465 approximately equal purity; both methods also resulted in identical Ruc chaperone activity
466 upon oxidation of the protein. In the first method, untagged Ruc was purified from strain
467 ER2566. A 500 ml culture was grown at 37ºC with shaking to an OD_{600} of 0.5, and then
468 cooled to room temperature. 1 mM isopropyl β-D-thiogalactopyranoside (IPTG) was
469 added, and the culture was grown further at 30ºC with shaking for five hours. Bacteria
470 were collected by centrifugation, resuspended in 25 ml of 50 mM Tris, pH 8.0, and lysed
471 by sonication. After removing insoluble material by centrifugation, ammonium sulfate was
472 added to the lysate to 70% w/v, and the suspension was stirred for 30 minutes at 4ºC to
473 precipitate proteins. The precipitate was collected by centrifugation, resuspended in 3 ml
474 of 50 mM Tris, pH 8.0, and dialyzed against four liters of the same buffer at 4ºC overnight
475 to remove residual ammonium sulfate and dissolve proteins. Ruc has a predicted
476 isoelectric point of approximately 9, and was therefore one of the few positively-charged
477 proteins in the bacterial protein extract. Taking advantage of this fact, Ruc was purified to
478 homogeneity by passing the protein extract over a Q Sepharose anion exchange column
479 (GE); Ruc immediately exited the column in flow-through fractions. To ensure that the
480 protein was fully reduced after purification, we treated Ruc with 5 mM DTT for 30 minutes
481 at 30ºC. An Amicon centrifugal filter unit (Millipore) was used to thoroughly buffer-
482 exchange the protein into 50 mM HEPES, pH 7.5. The complete removal of DTT was
483 confirmed by measuring the presence of DTT in the filter flowthrough using Ellman's

reagent (Thermo Scientific) according to the manufacturer's instructions. The final protein preparation (Ruc_{red}) was stored in the same buffer at -20ºC.

The second method of preparing Ruc from *E. coli* used a cleavable affinity tag, and was also used to obtain Ruc_{Nterm}, $Ruc_{C8S,C11S}$, and $Ruc_{C29S,C32S}$. His_6-SUMO-Ruc, His_6-SUMO-Ruc_{Nterm}, His_6-SUMO-$Ruc_{C8S,C11S}$, and His_6-SUMO-$Ruc_{C29S,C32S}$ were each purified from strain BL21(DE3) in the following manner. A 500 ml culture was grown at 37ºC with shaking to an OD_{600} of 0.3 to 0.4, then transferred to a 25ºC shaking incubator and grown to an OD_{600} of 0.5. 1 mM IPTG was added, and the culture were further grown for 5 hours. Purified protein was prepared from bacteria using Ni-NTA resin, and then exchanged into a SUMO cleavage buffer of 50 mM Tris, 150 mM NaCl, 2 mM dithiothrietol (DTT), pH 8.0. A 1:100 volume of purified His_6-Ulp1 (SUMO protease) was added, and the reaction was incubated for 30 minutes at 30ºC. His_6-Ulp1 and His_6-SUMO were then removed by incubating the mixture with Ni-NTA resin and saving the supernatant fraction; clearance of tagged protein was performed twice to yield pure, native Ruc and truncation or substitution variants. Proteins were buffer-exchanged into TBS buffer (50 mM Tris, 150 mM NaCl, pH 8.0) using centrifugal filters, and the absence of residual DTT was confirmed using Ellman's reagent. The final protein preparations (Ruc_{red}, $Ruc_{Nterm-red}$, $Ruc_{C8S,C11S-red}$, and $Ruc_{C29S,C32S-red}$) were stored in TBS at -20ºC.

M. tuberculosis DnaK, DnaJ2, and GrpE were prepared by removing the affinity tags from His_6-SUMO-DnaK, His_6-SUMO-DnaJ2, and His_6-SUMO-GrpE in the same manner as described for His_6-SUMO-Ruc, except that the native proteins were buffer-exchanged into 50 mM Tris, 150 mM KCl, 20 mM MgCl2, 2 mM DTT, pH 7.5 before storage at -20ºC.

Separation of proteins in *in vitro* assays and in *M. tuberculosis* lysates was performed using 15% sodium dodecyl sulfate-polyacrylamide (SDS-PAGE) gels, with the following exceptions: for Figures 1B and 1C, anykD Mini-PROTEAN TGX precast protein gels (Bio-Rad) were used. Bio-Safe Coomassie Stain (Bio-Rad) was used to stain gels. For preparing samples for SDS-PAGE gels in Figures 3A and 4B, purified proteins were mixed with 4 × non-reducing SDS buffer (250 mM Tris pH 6.8, 2% SDS, 40% glycerol, 1% bromophenol blue) to a 1 × final concentration, and samples were boiled for five minutes. For lane 3 in Figure 3A, DTT was added to the sample to a 2 mM final concentration prior to boiling. For immunoblots, proteins were transferred from protein gels to nitrocellulose membranes (GE Amersham), and analyzed by immunoblotting as indicated. Due to Ruc's high isoelectric point, Ruc was transferred to membranes using 100 mM N-cyclohexyl-3-aminopropanesulfonic acid (CAPS) buffer in 10% methanol. In Figures 1B and 1C, Ruc and PrcB immunoblots were from the same membrane. For detecting *M. tuberculosis* DnaK we used a monoclonal antibody from BEI Resources (NR-13609) at a concentration of 1:1000 in 3% BSA in 25 mM Tris-Cl/125 mM NaCl/0.05% Tween 20 buffer (TBST). Polyclonal antibodies against PrcB (23) and Ruc were used similarly. Secondary antibodies HRP-conjugated goat anti-rabbit IgG F(ab')2 and HRP-conjugated anti-mouse IgG(H+L) were purchased from Thermo Fisher Scientific. All antibodies were made in TBST with 3% BSA. Immunoblots were developed using SuperSignal West Pico PLUS chemiluminescent substrate (Thermo Fisher Scientific) and imaged using a Bio-Rad ChemiDoc system.

Preparation of *M. tuberculosis* extracts for immunoblotting. *M. tuberculosis* cultures were grown to an OD_{580} of 0.3. Equal amounts of bacteria were harvested by centrifugation, resuspended in TBS, and transferred to a tube containing 250 µl of 0.1 mm zirconia beads (BioSpec Products). Bacteria were lysed using a mechanical bead-beater (BioSpec Products). Whole lysates were mixed with 4 × reducing SDS sample buffer (250 mM Tris pH 6.8, 2% SDS, 20% 2-mercaptoethanol, 40% glycerol, 1% bromophenol blue) to a 1 × final concentration, and samples were boiled for 5 minutes. For preparing lysates from *M. tuberculosis* grown in 7H9, which contains BSA, an additional wash step with PBS-T was done prior to resuspension of bacteria in lysis buffer.

Mouse infections. Six to eight-week old female C57BL6/J mice (Jackson Laboratories) were each infected with ~200-400 *M. tuberculosis* bacilli by the aerosol infection route. Bacterial burden in organs was determined as previously described (57); briefly, at the time points indicated in the text, lung pairs and spleens were harvested from 3 to 5 mice, and were each homogenized and plated on 7H11 agar to determine CFU per organ. All procedures were performed with the approval of the New York University Institutional Animal Care and Use Committee.

Preparation of Ruc_{ox} and $Ruc_{Nterm\text{-}ox}$. 8.8 M H_2O_2 stock solution, stored at -20ºC, was diluted to 200 mM in deionized water just prior to the oxidation reaction. 100 µM Ruc_{red} or $Ruc_{Nterm\text{-}red}$ were incubated at 37ºC; for 3 min, after which 50 µM of copper chloride was added, followed by 2 mM H_2O_2. The reaction was incubated for 10 minutes; H_2O_2 and copper chloride were removed using a Zeba Spin 7K MWCO desalting centrifuge column

552 (Fisher Scientific) pre-equilibrated with the original Ruc_{red} storage buffer, according to the
553 manufacturer's instructions. Treatment of Ruc with 2 mM DEANO (Sigma-Aldrich) or
554 NaOCl (Figure S1B) was performed identically, except that Ruc was treated for 20
555 minutes (NaOCl) or two hours (DEANO) as described for Hsp33 (58).
556
557 **Spectrophotometric detection of zinc in Ruc preparations.** Quantification of the zinc
558 coordinated by Ruc cysteines was performed using 4-(2-pyridylazo)resorcinol (PAR)
559 using a previously established method (32, 59), except that zinc-cysteine complexes were
560 disrupted using N-ethylmaleimide (NEM) (Pierce) according to the manufacturer's
561 instructions. 25 µM Ruc was mixed with 100 µM PAR either in the absence or presence
562 of 2 mM NEM. Reactions were incubated at room temperature for 1 hour. $Zn(PAR)_2$
563 complexes were detected by A_{500} using a NanoDrop spectrophotometer. To obtain a
564 precise concentration of zinc in protein preparations, serial dilutions of zinc sulfate
565 prepared in matched buffers (with or without NEM) were used to prepare standard curves.
566 Three technical replicates were performed for each condition.
567
568 **Metal analysis of Ruc preparations using inductively-coupled plasma mass**
569 **spectrometry (ICP-MS).** Elemental quantification on purified Ruc with and without NEM
570 and a buffer control was performed using an Agilent 7700 inductively coupled plasma
571 mass spectrometer (Agilent, Santa Clara, CA) attached to a Teledyne CETAC
572 Technologies ASX-560 autosampler (Teledyne CETAC Technologies, Omaha, NE). The
573 following settings were fixed for the analysis Cell Entrance = -40 V, Cell Exit = -60 V, Plate
574 Bias = -60 V, OctP Bias = -18 V, and collision cell Helium Flow = 4.5 mL/min. Optimal

voltages for Extract 2, Omega Bias, Omega Lens, OctP RF, and Deflect were determined empirically before each sample set was analyzed. Element calibration curves were generated using ARISTAR ICP Standard Mix (VWR, Radnor, PA). Samples were introduced by peristaltic pump with 0.5 mm internal diameter tubing through a MicroMist borosilicate glass nebulizer (Agilent). Samples were initially up taken at 0.5 rps for 30 s followed by 30 s at 0.1 rps to stabilize the signal. Samples were analyzed in Spectrum mode at 0.1 rps collecting three points across each peak and performing three replicates of 100 sweeps for each element analyzed. Sampling probe and tubing were rinsed for 20 s at 0.5 rps with 2 % nitric acid between every sample. Data were acquired and analyzed using the Agilent Mass Hunter Workstation Software version A.01.02.

Circular dichroism (CD) spectrophotometry. CD measurements were performed using a Jasco J-1500 CD spectrophotometer as per the manufacturer's instructions. To prepare samples, Ruc was buffer-exchanged into 20 mM KH_2PO_4, pH 7.5, diluted to 20 µM, and transferred to a quartz cuvette. The spectrophotometer parameters were set as follows: CD scale 200 mdeg/1.0 dOD, integration time 1 second, bandwidth 1 nm. The voltage was monitored simultaneously and remained below 700 V.

Luciferase aggregation and refolding assays. The chaperone activity of Ruc was measured by testing its ability to limit the aggregation of heat-denatured luciferase, a previously established method (15, 37). For experiments in Figures 4A, 4C, and 4E, aggregation was determined by measuring absorbance at 350 nm (A_{350}) (60, 61). Firefly luciferase (Promega) was diluted to 2 µM in TBS and mixed in a microcentrifuge tube with

598 concentrations of Ruc indicated in the text and figures, or TBS alone, to a final volume of
599 20 µl. The tube was then incubated in a 45ºC heat block. Immediately before incubation
600 and at the indicated times, a 2 µl volume was removed and A_{350} was measured using a
601 NanoDrop spectrophotometer. Aggregation assays were performed using three technical
602 replicates per condition. For the experiment in Figure S1A, luciferase aggregation was
603 measured using light scattering as previously described (15).

604 Refolding of heat-denatured luciferase by *M. tuberculosis* DnaKJE was performed
605 using a protocol adapted from (11). *M. tuberculosis* encodes two DnaJ homologs, DnaJ1
606 and DnaJ2, which both promote DnaK-mediated protein folding *in vitro* (11); DnaJ2 was
607 used in this study because we found that DnaJ1 exhibited poor solubility when purified
608 from *E. coli*. For the denaturation step, luciferase was diluted to 0.1 µM in TBS, either
609 alone or mixed with 4 µM Ruc_{red} or Ruc_{ox}, in glass vials. Denaturation was performed by
610 placing vials in a 45ºC water bath for 20 minutes. For the refolding step, we used glass-
611 coated 96-well plates in which 5 µl of denaturation reaction was mixed with 15 µl of
612 refolding reaction buffer [50 mM Tris pH 7.5, 150 mM KCl, 20 mM $MgCl_2$, 2 mM DTT, 1
613 mg/ml BSA (Sigma-Aldrich), 2 mM Mg^{2+}-ATP] or refolding reaction buffer containing 4 µM
614 DnaK, 2 µM DnaJ2, and 2 µM GrpE. Plates were incubated at 25ºC. Luciferase activity
615 was measured immediately upon initiating the refolding step (0 minutes) and at all other
616 time points indicated in Figure 5A by transferring 2 µl of each reaction into a white opaque
617 96-well plate and adding 100 µl of luciferase assay mix (100 mM KH_2PO_4 pH 7.5, 25 mM
618 glycyl glycine, 0.2 mM EDTA, 2 mM Mg^{2+}-ATP, 0.5 mg/ml BSA, 70 µM luciferine).
619 Luminescence was measured using a plate reader (PerkinElmer EnVision). For
620 calculating the percent of native luciferase activity for all reactions at each time point, a

control reaction was included in which 0.1 µM luciferase was diluted into TBS in a glass vial but kept at 4ºC, rather than heated, during the denaturation step. This control reaction was mixed with refolding reaction buffer as described above, and luminescence was measured at each time point in Figure 5A to determine 100% native luciferase activity.

Tandem affinity purification of *M. tuberculosis* proteins. Purifications of TAP-tagged proteins from *M. tuberculosis* were performed under low-salt conditions as described (62). The following changes were made to the protocol: 100 µl of packed Ni-NTA beads and 100 µl of M2 anti-FLAG affinity gel were used; 100 µl of 100 µM 3X FLAG peptide was used for the final elution. For capturing Ruc_{TAP} interactions with other *M. tuberculosis* proteins, *M. tuberculosis* lysates were incubated at 45ºC for 10 minutes either in the absence (Figure 5C, lane 1) or presence (Figure 5C, lane 2) of 2 mM H_2O_2 and 50 µM $CuCl_2$; purifications were subsequently performed as described above. Samples were boiled in 4 × reducing SDS sample buffer prior to running SDS-PAGE gels.

Protein mass spectrometry. To identify of the ~70 kDa protein pulled down by Ruc_{TAP} (Figure 5B), the band was excised from a SDS-PAGE gel and processed as previously described (63). To determine the identity of proteins enriched in Ruc_{TAP} purifications under oxidizing conditions (Figure 5C; Table S2), Ruc_{TAP} purifications under native or oxidizing conditions were performed in three biological replicates. Affinity purified samples were reduced, alkylated, digested with trypsin and desalted as previously described (23, 63). The peptide eluates in all cases were concentrated in the SpeedVac and stored at -80°C. Aliquots of each sample were loaded onto a trap column (Acclaim® PepMap 100

pre-column, 75 µm × 2 cm, C18, 3 µm, 100 Å, Thermo Scientific) connected to an analytical column (EASY-Spray column, 50 m × 75 µm ID, PepMap RSLC C18, 2 µm, 100 Å, Thermo Scientific) using the autosampler of an Easy nLC 1000 (Thermo Scientific) with solvent A consisting of 2% acetonitrile in 0.5% acetic acid and solvent B consisting of 80% acetonitrile in 0.5% acetic acid. The peptide mixture was gradient eluted into the Orbitrap QExactive HF-X mass spectrometer (Thermo Scientific) using the following gradient: 5%-35% solvent B in 120 min, 35% -45% solvent B in 10 min, followed by 45%-100% solvent B in 20 min. The full scan was acquired with a resolution of 45,000 (@ m/z 200), a target value of 3e6 and a maximum ion time of 45 ms. Following each full MS scan, twenty data-dependent MS/MS spectra were acquired. The MS/MS spectra were collected with a resolution of 15,000 an AGC target of 1e5, maximum ion time of 120ms, one microscan, 2m/z isolation window, fixed first mass of 150 m/z, dynamic exclusion of 30 sec, and Normalized Collision Energy (NCE) of 27. All acquired MS2 spectra were searched against a UniProt *M. tuberculosis* H37Rv database including common contaminant proteins using Sequest HT within Proteome Discoverer 1.4 (Thermo Fisher Scientific). The search parameters were as follows: precursor mass tolerance ±10 ppm, fragment mass tolerance ±0.02 Da, digestion parameters trypsin allowing two missed cleavages, fixed modification of carbamidomethyl on cysteine, variable modification of oxidation on methionine, and variable modification of deamidation on glutamine and asparagine and a 1% peptide and protein FDR searched against a decoy database. The results were filtered to only include proteins identified by at least two unique peptides. Fold change analysis was performed for the Ruc_{TAP} purifications using the ratios of PSMs in oxidized to the PSMs in the native affinity purified samples using the SAINT algorithm

667 (64). SAINT scores were used to calculate the false discovery rate (FDR); proteins whose
668 SAINT score yielded an FDR of 5% or lower were considered statistically significant and
669 are highlighted in Table S2.
670
671 **Measurement of *M. tuberculosis* susceptibility to oxidants.** *M. tuberculosis* was
672 grown in 7H9c to an OD_{580} of 0.5 at 37ºC, centrifuged and resuspended in fresh 7H9c,
673 and spun at 500 × g to remove clumps of bacteria. Supernatants were then diluted to an
674 OD_{580} of 0.025, transferred to 96-well plates, and incubated at 45ºC for four hours to
675 induce Ruc production. Afterwards, *M. tuberculosis* strains were subjected to oxidizing
676 reagents and inoculated onto 7H11 agar as described in the legend for Fig. S3.
677
678 **Computational analyses.** Iterative sequence profile searches were performed to recover
679 Ruc sequence homologs using the PSI-BLAST program (65). Searches were either run
680 against the non-redundant (nr) protein database of the National Center for Biotechnology
681 Information (NCBI), or a custom database of 7423 complete prokaryotic genomes
682 extracted from the NCBI Refseq database (66). The latter was used for phyletic profile
683 analyses (Table 2). Contextual information from prokaryotic gene neighborhoods was
684 retrieved using a Perl script that extracts the upstream and downstream genes of a query
685 gene from a GenBank genome file. This was followed by clustering of proteins using the
686 BLASTCLUST program (ftp://ftp.ncbi.nih.gov/blast/documents/blastclust.html) to identify
687 conserved gene-neighborhoods. Analysis and visualization of phyletic patterns was
688 performed using the R language.
689

690 **Acknowledgments**

691 We thank C. Nathan and K. Burns-Huang for providing strains and technical advice. This
692 work was supported by NIH grants AI088075 and AI144851 awarded to K.H.D. S.H.B
693 was supported by NIH grant T32 AT007180. S.H.B. also received support from the Jan
694 T. Vilcek Endowed Fellowship Fund. E.P.S. received support from AI150701 and
695 AI069233. K.U. and U.J. thank the DFG Priority Program SPP 1710 (Schw823/3-2). L.M.I.
696 and L.A. are supported by the intramural funds of the National Library of Medicine, NIH.
697 The mass spectrometry experiments were in part supported by the NYU Grossman
698 School of Medicine.

699

700 **Author contributions**

701 S.H.B., K.U., A.D., B.U., W.B., E.P.S., L.I., L. A., U.J. and K.H.D. designed research;
702 S.H.B., K.U., A.D., W.B., L.M.I., and L.A. performed research; S.H.B, K.H.D., and L.A.
703 wrote the manuscript.

704

705

706

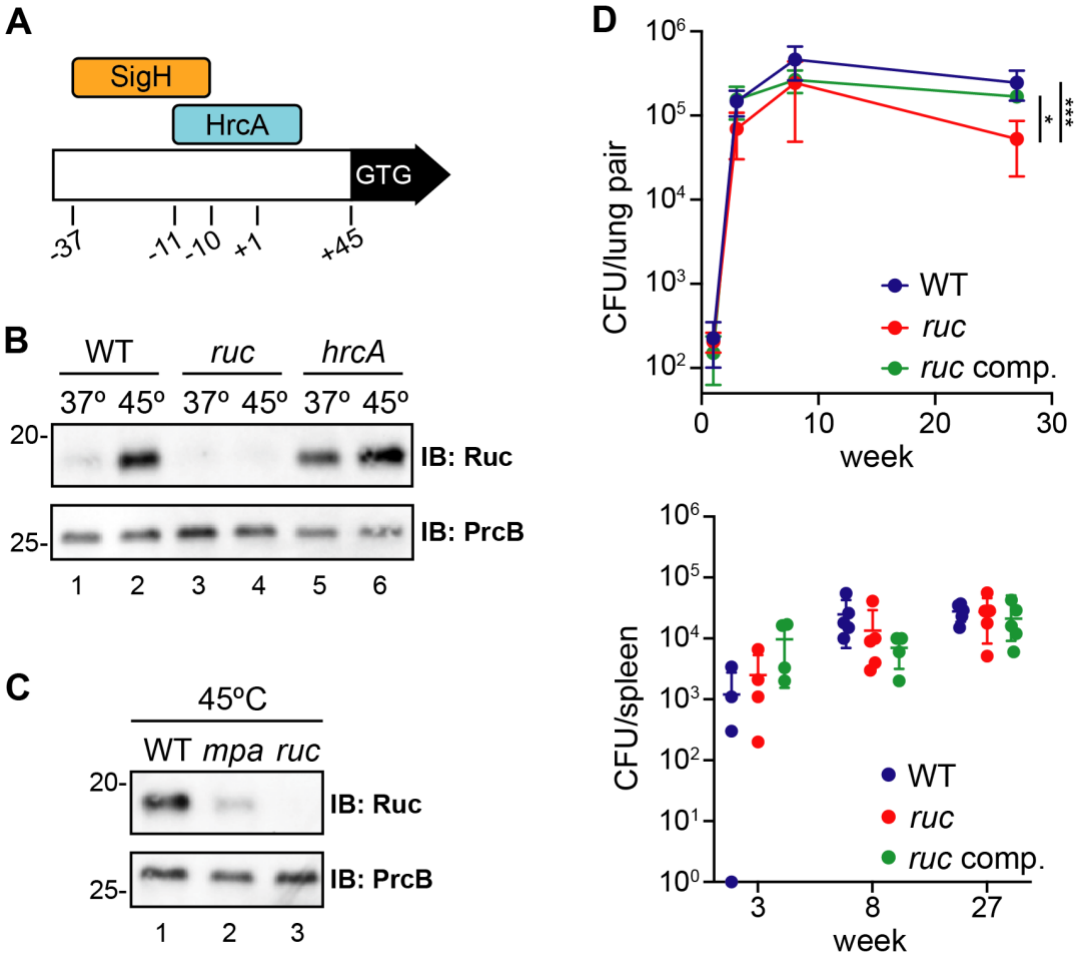

707 **Fig. 1. *M. tuberculosis* Ruc is a heat shock-inducible, HrcA- and Mpa-regulated**
708 **small protein**. **(A)** Illustration of the *ruc* control region in *M. tuberculosis*. The position of
709 the *ruc* transcriptional start site (+1), as well as the binding sites of sigma factor SigH and
710 repressor HrcA are shown relative to the +1 (24, 25). A second +1 was identified 19
711 nucleotides upstream of the +1 shown here (67). **(B)** WT (MHD1), *ruc* (MHD1384), and
712 *hrcA* (MHD1384) *M. tuberculosis* strains were incubated at 37ºC or 45ºC, and Ruc
713 abundance was assessed in bacterial lysates by immunoblot (IB). Immunoblotting for
714 PrcB was used as a loading control. **(C)** WT, *mpa* (MHD149), and *ruc* strains analyzed
715 as in panel (B). **(D)** Mice were infected with WT with empty vector (MHD1385), *ruc* with
716 empty vector (MHD1393), or *ruc* complemented with pMV306kan-*ruc* (MHD1394) *M.*
717 *tuberculosis* strains, and bacterial burden in the lungs (top panel) and spleen (bottom
718 panel) was determined at day 1 or at weeks 3, 8, and 27. Statistical significance was
719 determined using one-way ANOVA; ***, $p < 0.001$; *, $p < 0.05$. Significant differences in
720 lung bacterial burden are shown for 27 weeks after infection; all other time points were
721 determined to be not significant ($p > 0.05$).
722

723

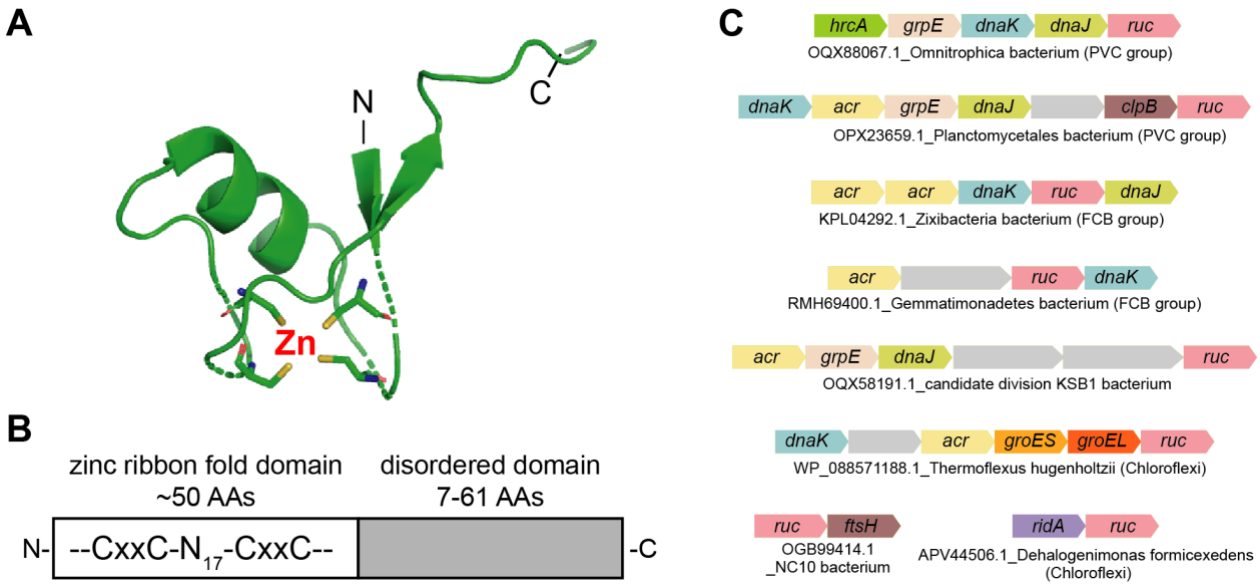

724

725 **Fig. 2. Ruc contains a putative zinc-binding domain with a disordered C-terminus,**
726 **and co-occurs with proteostasis genes in diverse bacterial lineages. (A)** Predicted
727 structure of the N-terminal region of *M. tuberculosis* Ruc (residues 5-48) based on Phyre2
728 predictive modeling (30). The four cysteines in Ruc are represented as sticks, with the
729 thiol groups shown in yellow. The position of a predicted zinc ion is also shown. **(B)**
730 Illustration of the conserved features of Ruc. x, unspecified amino acid; N_{17}, region 17
731 residues in length. **(C)** Genetic loci containing *ruc* with neighboring genes encoding
732 chaperones, proteases, or chaperone-associated transcriptional regulators.
733 Representatives of the phyletic groups PVC (Plantomycetes, Verrucomicrobia,
734 Chlamydiae) and FCB (Fibrobacteres, Chlorobi, Bacteroidetes), as well as members of
735 Chloroflexi and unclassified phyla, are shown. Genes are represented by the NCBI
736 GenBank database accession number of the *ruc* gene followed by the species name and
737 bacterial clade in bracket (if known).

738

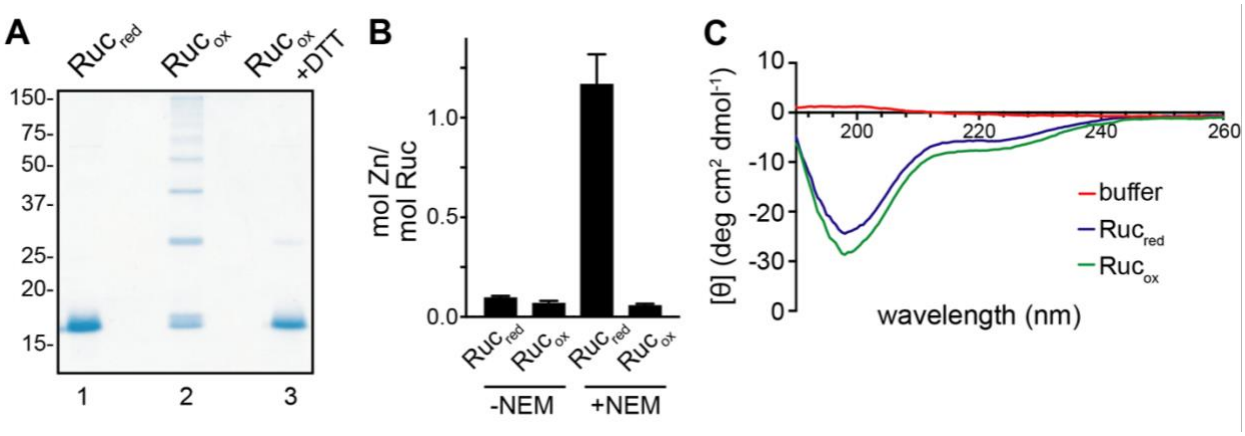

739 **Fig. 3. Ruc contains redox-active cysteines that coordinate a single zinc atom, and**
740 **is an intrinsically disordered protein. (A)** Reduced Ruc (Ruc_{red}), oxidized Ruc (Ruc_{ox}),
741 or Ruc_{ox} treated with the thiol-reducing agent dithiothrietol (DTT) were separated on an
742 SDS-PAGE gel and stained with Coomassie brilliant blue. **(B)** Zinc coordination by Ruc_{red}
743 or Ruc_{ox} was quantified in the absence or presence of N-ethylmaleimide (NEM), which
744 modifies cysteines. Zinc concentrations were measured spectrophotometrically using the
745 metal chelator 4-(2-pyridylazo)resorcinol (PAR) (see Materials and Methods for details).
746 **(C)** Assessment of Ruc secondary structure using circular dichroism, with degrees of
747 ellipticity [θ] plotted by wavelength.

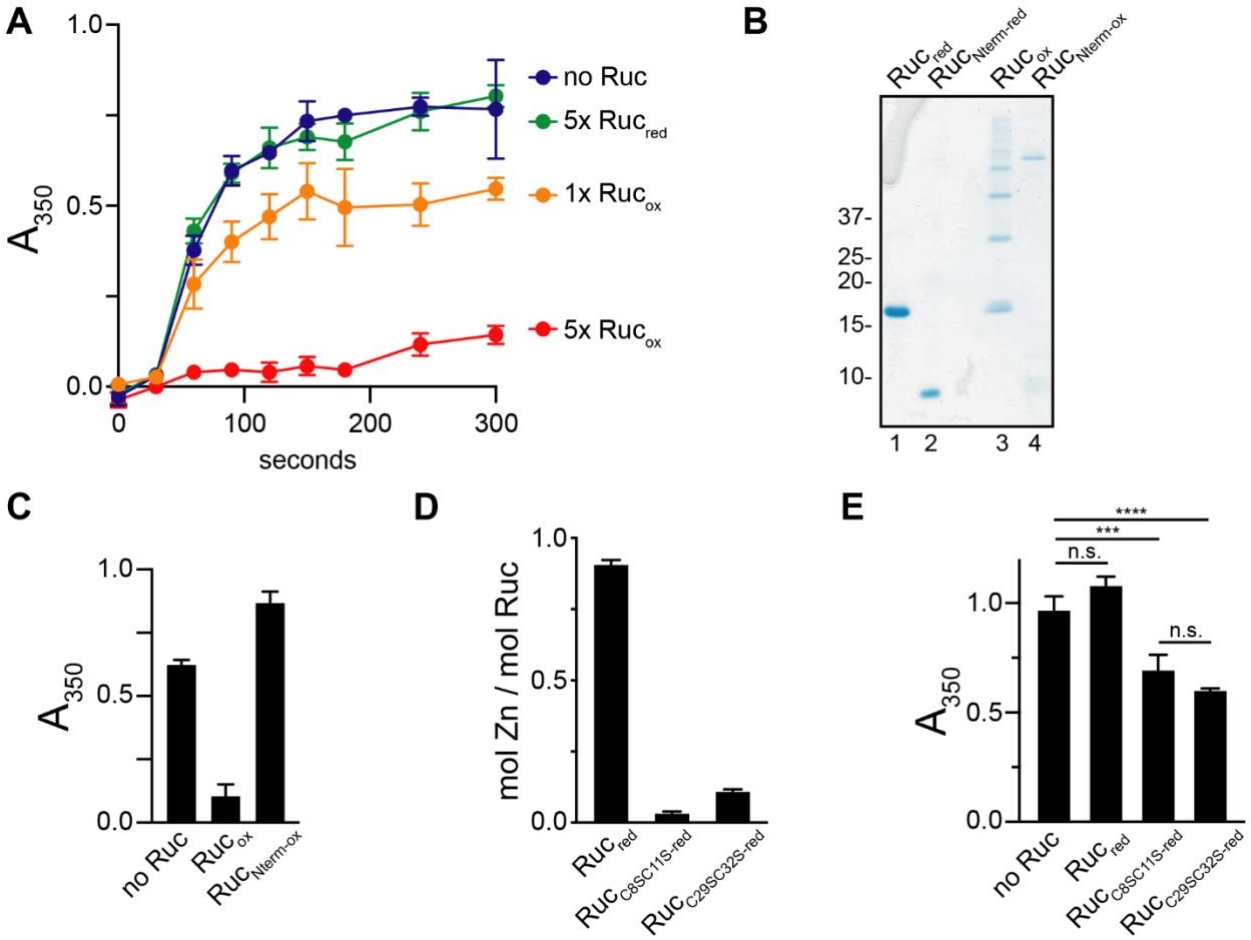

Fig. 4. Oxidized Ruc inhibits protein aggregation. (A) Aggregation of luciferase upon heat denaturation. Luciferase was incubated at 45ºC either alone or in the presence of a five-fold molar excess (5x) of Ruc_{red}, 5x Ruc_{ox}, or an equimolar concentration (1x) of Ruc_{ox}. Aggregation was assessed by absorbance at 350 nm (A_{350}). The difference in aggregation between no Ruc and 1x Ruc_{ox} or 5x Ruc_{ox} conditions was statistically significant (paired *t*-test, $P < 0.01$), while no significant difference was obtained with Ruc_{red}. **(B)** Ruc and Ruc_{Nterm} (comprising residues 1-49), in either a reduced or oxidized state, were separated on a Coomassie-stained SDS-PAGE gel. **(C)** Aggregation of heat-denatured luciferase as in (A), except only the 300 second time point is shown. Native Ruc_{ox} or $Ruc_{Nterm\text{-}ox}$ were incubated with luciferase in fivefold molar excess at 45ºC as indicated. **(D)** Quantification of zinc in native Ruc and Ruc cysteine-to-serine variants, as described for Figure 3B. NEM was included in all reactions. **(E)** Luciferase aggregation assay as in (C) to assess the activity of reduced Ruc cysteine-to-serine variants. Statistical significance was determined using one-way ANOVA; ****, $P < 0.0001$; ***, $P < 0.001$; n.s., not statistically significant ($P > 0.05$). All reactions were performed in triplicate.

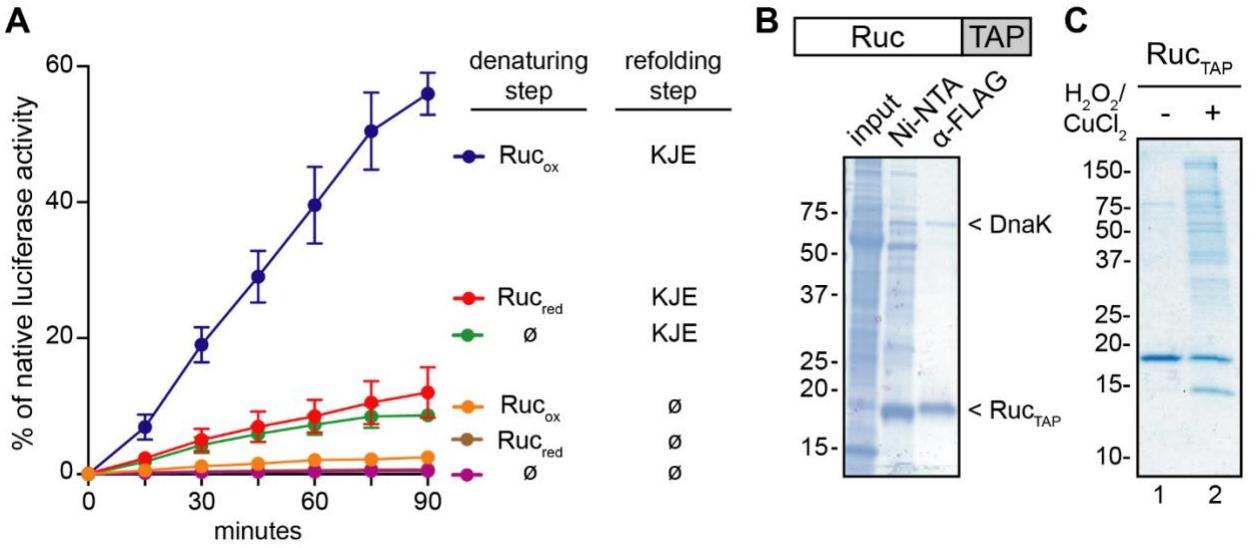

Fig. 5. Ruc promotes protein folding by the *M. tuberculosis* Hsp70 system and associates with many *M. tuberculosis* proteins. (A) Luciferase was denatured at 45ºC in the presence of either Ruc_{red}, Ruc_{ox}, or a buffer control (ø). Reactions were then cooled to 25ºC and incubated either with DnaK, DnaJ2, and GrpE (KJE). Refolding of denatured luciferase was determined by measuring luciferase activity at the indicated time points following addition of KJE or buffer. As a control, native luciferase activity was measured at each time point by incubating non-denatured luciferase in the same buffer for the same duration (see Materials and Methods for a detailed protocol). Data shown are the result of three independent experiments comparing each condition. **(B)** Ruc containing a C-terminal hexahistidine-FLAG tandem affinity purification tag (Ruc_{TAP}, illustrated above) was purified from *M. tuberculosis* strain MHD1541. A two-step purification was performed on soluble *M. tuberculosis* lysates (input) using Ni-NTA resin followed by FLAG antibody gel (α-FLAG). The identity of DnaK was determined using mass spectrometry (see Materials and Methods) and immunoblotting (see Figure S2A). **(C)** RucTAP was purified from *M. tuberculosis* as in (B), except that input lysates were subjected to oxidation (H_2O_2 and $CuCl_2$ treatment) or no treatment prior to purification. The final α-FLAG-purified material is shown. For (B) and (C), samples were separated on SDS-PAGE gels under reducing conditions.

Fig. 6. Model of Ruc chaperone activity in *M. tuberculosis*. From left to right; under the steady-state reducing conditions of the cytoplasm, Ruc coordinates zinc and is inactive; upon oxidation of Ruc cysteines, zinc is displaced and Ruc binds to unfolded proteins; a Ruc client protein is transferred to the Hsp70 system for refolding into its native conformation.

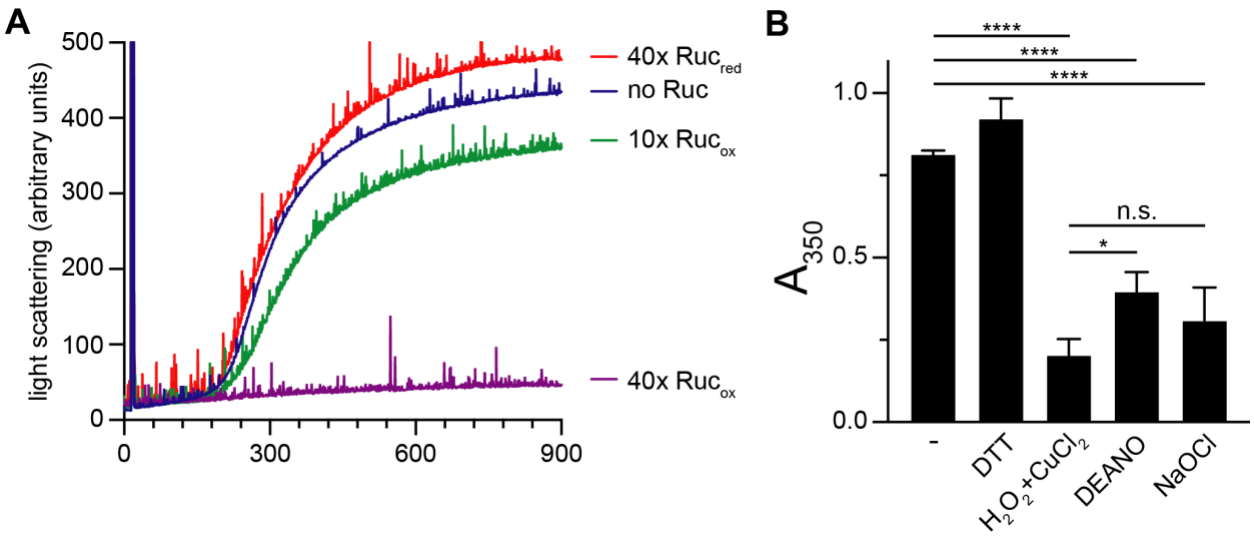

Fig. S1. Ruc$_{ox}$ inhibits protein aggregation and is activated by multiple oxidants. **(A)** Measurement of denatured luciferase aggregation using light scattering spectrophotometry. Luciferase was incubated alone, in the presence of a 40-fold (40x) or 10-fold (10x) molar excess of Ruc$_{ox}$, or a 40-fold molar excess of Ruc$_{red}$. **(B)** Measurement of denatured luciferase aggregation using absorbance at 350 nm (A_{350}). Luciferase was incubated at 45ºC for 5 minutes either alone (-) or in the presence of Ruc pre-treated with 2 mM DTT, 2 mM H_2O_2 with 0.5 mM $CuCl_2$, 2 mM diethylamine NONOate (DEANO, a nitric oxide donor), or 2 mM sodium hypochlorite (NaOCl). Data in (A) is representative of two independent experiments; (B) was performed using three replicates per condition. Statistical significance was determined using one-way ANOVA; ****, $p < 0.0001$; *, $p < 0.05$; n.s., not statistically significant ($p > 0.05$).

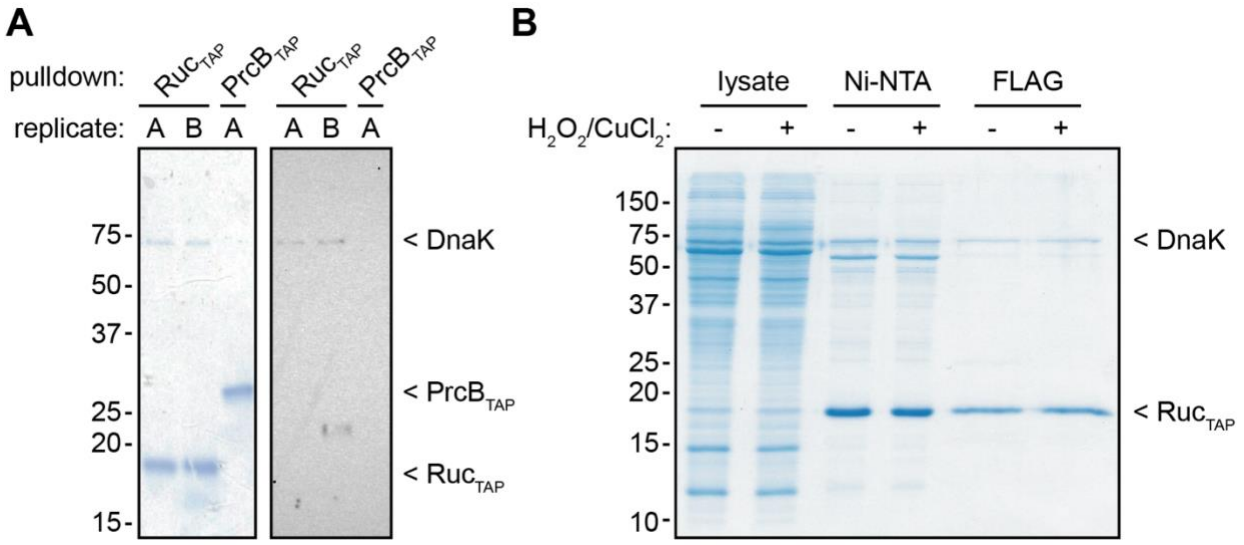

Fig. S2. Ruc$_{TAP}$ co-purifies with DnaK, and subjecting *M. tuberculosis* to oxidation does not affect Ruc$_{TAP}$ purification. (A) Ruc$_{TAP}$ or PrcB$_{TAP}$ (a control, TAP-tagged protein) purifications from *M. tuberculosis* were separated on an SDS-PAGE gel and either stained with Coomassie brilliant blue (left) or analyzed by immunoblotting with a monoclonal antibody against *M. tuberculosis* DnaK (right). **(B)** Ruc$_{TAP}$ was purified in two steps (Ni-NTA resin followed by α-FLAG affinity gel) from *M. tuberculosis* cultures (strain MHD1541) that were either untreated or treated with a sublethal concentration of oxidants (0.625 mM H_2O_2 with 16 nmol $CuCl_2$) for 30 minutes at 45ºC.

819

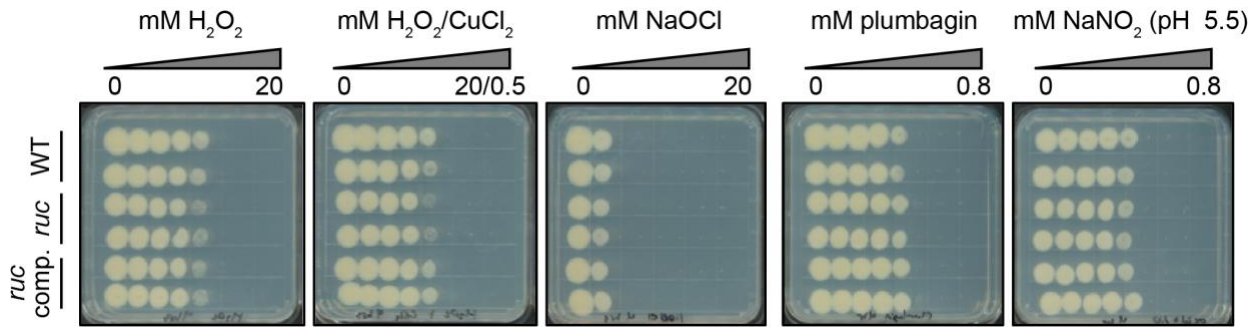

820 **Figure S3. WT and *ruc* mutant strains are equally sensitive to oxidants.** The
821 approximate lethal dose of the indicated oxidizing agents (above) on *M. tuberculosis*
822 strains (left; MHD1385, MHD1393, and MHD1394 are represented). A series of two-fold
823 serial dilutions of each oxidant was added to *M. tuberculosis* at the final concentrations
824 shown; cultures were incubated along with oxidants at 45ºC for four hours. Afterwards,
825 cultures were spot-plated onto solid agar media, and plates were incubated at 37ºC for
826 two weeks to assess surviving bacteria.

Table 1. Strains, plasmids and primers used in this work.

***M. tuberculosis* strains**

Strain	Relevant genotype or description	Source or reference
MHD1	Wild-type H37Rv	American Type Culture Collection (ATCC) #25618
MHD1383	Hyg_R; Δ*hrcA*::*hyg*	(23)
MHD1384	Hyg_R; Δ*ruc*::*hyg* (deletion-disruption mutation of Rv0991c)	(23)
MHD149	Hyg_R; Δ*mpa*::*hyg*	(57)
MHD1541	Hyg_R; H37Rv, pOLYG-*ruc*-TAP	This study
MHD1385	Kan_R; H37Rv, pMV306kan	This study
MHD1393	Kan_R, Hyg_R; MHD1384, pMV306kan	This study
MHD1394	Kan_R, Hyg_R; MHD1384, pMV306kan-*ruc*	This study

***E. coli* strains**

Strain	Relevant genotype or description	Source or reference
DH5α	*supE44* Δλ*acU169 (φ80 lacZΔM15) hsdR17 recA1 endA1 gyrA96 thi-1 relA1* (Nal_R)	Gibco
ER2566	F- λ- f*huA2* [*lon*] *ompT lacZ::T7 geneI gal sulA11* Δ(m*crC-mrr*)1*14::IS10 R(mcr-73*::miniTn*10*)2 *R*(*zgb-210*::Tn*10*)1 (tetS) *endA1* [*dcm*]	(68)
BL21 (DE3)	F_- *ompT gal dcm lon hsdS*$_B$($r_{B-}m_{B-}$) λ(DE3 [*lacI lacUV5-T7p07 ind1 sam7 nin5*] [*malB*$^+$]$_{K-12}$(λ_S)	New England Biolabs

Plasmids

Plasmid	Relevant genotype or description	Source or reference
pET24b(+)	Kan_R; for inducible production of recombinant protein in *E. coli*	Novagen

pET24b(+)-Rv0991c-his6	Kan_R; for production of recombinant Ruc with C-terminal His_6 (Ruc-His_6)	This study
pAJD107	Amp_R; contains multiple restriction sites for cloning	(69)
pAJD107-Rv0991c	Amp_R; for making the *ruc* expression vector	This study
pAJD107-Rv0991c-C8SC11S	Amp_R; for cloning HisSUMO-*ruc*-C8SC11S expression vector	This study
pET24b(+)-Rv0991c	Kan_R; for production of recombinant, native Ruc	This study
pET24b(+)-Ruc-C8,11S	Kan_R; for cloning `HisSUMO-*ruc*-C8SC11S expression vector	This study
pEcTL02	Amp_R; for purification of *M. tuberculosis* ClpB with N-terminal His_6-SUMO from *E. coli*	(11)
pEcTL04	Amp_R; for purification of *M. tuberculosis* DnaJ2 with N-terminal His_6-SUMO from *E. coli*	(11)
pEcTL05	Amp_R; for purification of *M. tuberculosis* GrpE with N-terminal His_6-SUMO from *E. coli*	(11)
pEcTL06	Amp_R; for purification of *M. tuberculosis* DnaK with N-terminal His_6-SUMO from *E. coli*	(11)
pET24b(+)-HisSUMO-*ruc*	Kan_R; for purification of *M. tuberculosis* Ruc with N-terminal His_6-SUMO from *E. coli*	This study
pET24b(+)-HisSUMO-*ruc*-Nterm	Kan_R; for purification of *M. tuberculosis* Ruc_{Nterm} (amino acids 1 through 49) with N-terminal His_6-SUMO from *E. coli*	This study
pET24b(+)-HisSUMO-*ruc*-C8SC11S	Kan_R; for purification of *M. tuberculosis* $Ruc_{C8S,C11S}$ (containing cysteine to serine substitutions in residues 8 and 11) with N-terminal His_6-SUMO from *E. coli*	This study
pET24b(+)-HisSUMO-*ruc*-C29SC32S	Kan_R; for purification of *M. tuberculosis* $Ruc_{C29S,C32S}$ (containing cysteine to serine substitutions in residues 29 and 32) with N-terminal His_6-SUMO from *E. coli*	This study
pHYRS52	Amp_R; for purification of SUMO protease (*S. cerevisiae* Ulp1, amino acids 403-621) with N-terminal His_6 from *E. coli*	Addgene

pOLYG	Hyg$_R$; for overproduction of proteins in *M. tuberculosis*	(70)
pOLYG-Rv0991c-TAP	Hyg$_R$; for purification of Ruc with C-terminal hexahistidine-FLAG tandem affinity purification tag from *M. tuberculosis*	This study
pMV306kan	Kan$_R$; for integration into the L5 *attB* site of the *M. tuberculosis* chromosome	(71)
pMV306kan-Rv0991c	Kan$_R$; *ruc* complementation plasmid	This study

831 **Primers**

Primer name	Primer sequence
NdeI-Rv0991c-F	gatcCATATGccaacctacagctacgagtgcacc
HindIII-Rv0991c-R	gtagAAGCTTgacggccgcggcggcg
HindIII-Rv0991c-F	gtagAAGCTTtcgtctagtcgcggtggtgcg
XbaI-Rv0991c-R	ttatTCTAGAtcagacggccgcggcgg
XbaI-Rv0991c-TAP-R	gatcTCTAGAtcagtggtggtggtggtgctcgagtgcggccgccttatcgtcgtcatccttgtaatcgacggccgcgg cggcggttgtgga
BglII-Rv0991c-R	tagacAGATCTtcagacggccgcggcggcggttgt
SUMO-Ruc-soeR	ctcgtagctgtaggttggcaccccaccaatctgttctctgtgagcctc
SUMO-Ruc-soeF	gaggctcacagagaacagattggtggggtgccaacctacagctacgag
Ruc-KpnI-R	tataGGTACCtcagacggccgcggcggcggttgt
RucNterm-KpnI-R	tataGGTACCtcagcctttgaacaccacgccgaccgc
NdeI-Rv0991c-C8SC11S-F	GCGCCATATGCCAACCTACAGCTACGAGAGCACCCAGAGCGCCAACCGCTTCGAT GTTGTG
Rv0991c-C29SC32S-F	CCGACGATGCGCTGACCACGAGCGAGCGGAGTTCTGGCCGGCTGCGCAAGCTGT TC
Rv0991c-C29SC32S-R	GAACAGCTTGCGCAGCCGGCCAGAACTCCGCTCGCTCGTGGTCAGCGCATCGTCG G

T7-F	taatacgactcactataggg
T7-term	GCTAGTTATTGCTCAGCGG

832

833 **Table 2. Occurance of *ruc* in bacterial and archaeal phyla.**
834

Bacterial phylum (number of genomes)	**% genomes with *ruc***
gammaproteobacteria (923)	26.65
betaproteobacteria (333)	82.88
zetaproteobacteria (5)	80
alphaproteobacteria (469)	17.27
deltaproteobacteria (86)	86.05
proteobacteria (43)	74.42
thermodesulfobacteria (4)	100
spirochaetes (70)	48.57
deferribacteres (4)	100
chrysiogenetes (1)	100
nitrospirae (73)	86.3
acidobacteria (9)	100
elusimicrobia (3)	33.33
verrucomicrobia (74)	60.81
chlamydiae (43)	6.98
planctomycetes (18)	100
bacteroidetes (263)	1.9
chlorobi (263)	5.7
fibrobacteres (2)	0
gemmatimonadetes (3)	100
ignavibacteriae (2)	100
aquificae (15)	20
dictyoglomi (2)	100
thermotogae (29)	100
deinococcus-thermus (26)	100
synergistetes (5)	0
fusobacteria (16)	0
thermobaculum (1)	100
actinobacteria (497)	73.84
chloroflexi (22)	100
armatimonadetes (15)	73.33
tenericutes (124)	0
firmicutes (772)	8.94
cyanobacteria (127)	13.39
calditrichaeota (2)	100
unclassified bacteria (2565)	11.89
Archaeal phylum (number of genomes)	**% genomes with Ruc**

crenarchaeota (61)	1.64
euryarchaeota (187)	6.42
archaea (31)	3.23

835

836 **Table S1. ICP-MS analysis of Ruc metal binding.**

837 Excel spreadsheet in separate document

838 **Table S2. *M. tuberculosis* proteins that co-purified with Ruc$_{TAP}$.**

839 Excel spreadsheet in separate document

840

BIBLIOGRAPHY

1. **Mayer MP, Gierasch LM.** 2019. Recent advances in the structural and mechanistic aspects of Hsp70 molecular chaperones. J Biol Chem **294:**2085-2097.
2. **Laufen T, Mayer MP, Beisel C, Klostermeier D, Mogk A, Reinstein J, Bukau B.** 1999. Mechanism of regulation of Hsp70 chaperones by DnaJ cochaperones. *Proc. Nat. Acad. Sci. USA.* **96:**5452.
3. **Liberek K, Skowyra D, Zylicz M, Johnson C, Georgopoulos C.** 1991. The Escherichia coli DnaK chaperone, the 70-kDa heat shock protein eukaryotic equivalent, changes conformation upon ATP hydrolysis, thus triggering its dissociation from a bound target protein. *J Biol Chem* **266:**14491-14496.
4. **Harrison CJ, Hayer-Hartl M, Di Liberto M, Hartl F, Kuriyan J.** 1997. Crystal structure of the nucleotide exchange factor GrpE bound to the ATPase domain of the molecular chaperone DnaK. *Science* **276:**431-435.
5. **Veinger L, Diamant S, Buchner J, Goloubinoff P.** 1998. The Small Heat-shock Protein IbpB from Escherichia coli Stabilizes Stress-denatured Proteins for Subsequent Refolding by a Multichaperone Network. *J Biol Chem* **273:**11032-11037.
6. **Hoffmann JH, Linke K, Graf PCF, Lilie H, Jakob U.** 2004. Identification of a redox-regulated chaperone network. *EMBO J* **23:**160-168.
7. **Fernández-Fernández MR, Gragera M, Ochoa-Ibarrola L, Quintana-Gallardo L, Valpuesta JM.** 2017. Hsp70 – a master regulator in protein degradation. FEBS Letters **591:**2648-2660.
8. **Zolkiewski M.** 1999. ClpB Cooperates with DnaK, DnaJ, and GrpE in Suppressing Protein Aggregation: A Novel Multi-Chaperone System from *Escherichia coli*. *J Biol Chem* **274:**28083-28086.
9. **Goloubinoff P, Mogk A, Zvi AP, Tomoyasu T, Bukau B.** 1999. Sequential mechanism of solubilization and refolding of stable protein aggregates by a bichaperone network. *Proc. Nat. Acad. Sci. USA.* **96:**13732-13737.
10. **Weibezahn J, Tessarz P, Schlieker C, Zahn R, Maglica Z, Lee S, Zentgraf H, Weber-Ban EU, Dougan DA, Tsai FTF, Mogk A, Bukau B.** 2004. Thermotolerance Requires Refolding of Aggregated Proteins by Substrate Translocation through the Central Pore of ClpB. *Cell* **119:**653-665.
11. **Lupoli TJ, Fay A, Adura C, Glickman MS, Nathan CF.** 2016. Reconstitution of a Mycobacterium tuberculosis proteostasis network highlights essential cofactor interactions with chaperone DnaK. *Proc Natl Acad Sci U S A* 113:7947-7956.
12. **Haslbeck M, Weinkauf S, Buchner J.** 2018. Small heat shock proteins: Simplicity meets complexity. *J Biol Chem* 294:2121-2132.
13. **Ehrnsperger M, Gräber S, Gaestel M, Buchner J.** 1997. Binding of non-native protein to Hsp25 during heat shock creates a reservoir of folding intermediates for reactivation. *EMBO J* **16:**221-229.
14. **Żwirowski S, Kłosowska A, Obuchowski I, Nillegoda NB, Piróg A, Ziętkiewicz S, Bukau B, Mogk A, Liberek K.** 2017. Hsp70 displaces small heat shock proteins from aggregates to initiate protein refolding. *EMBO J* **36:**783-796.

15. **Jakob U, Muse W, Eser M, Bardwell JCA.** 1999. Chaperone Activity with a Redox Switch. *Cell* **96:**341-352.
16. **Graf PCF, Martinez-Yamout M, VanHaerents S, Lilie H, Dyson HJ, Jakob U.** 2004. Activation of the Redox-regulated Chaperone Hsp33 by Domain Unfolding. *J Biol Chem* **279:**20529-20538.
17. **Voth W, Schick M, Gates S, Li S, Vilardi F, Gostimskaya I, Southworth Daniel R, Schwappach B, Jakob U.** 2014. The Protein Targeting Factor Get3 Functions as ATP-Independent Chaperone under Oxidative Stress Conditions. *Mol. Cell* **56:**116-127.
18. **Graumann J, Lilie H, Tang X, Tucker KA, Hoffmann JH, Vijayalakshmi J, Saper M, Bardwell JCA, Jakob U.** 2001. Activation of the Redox-Regulated Molecular Chaperone Hsp33—A Two-Step Mechanism. *Structure* **9:**377-387.
19. **Winter J, Linke K, Jatzek A, Jakob U.** 2005. Severe Oxidative Stress Causes Inactivation of DnaK and Activation of the Redox-Regulated Chaperone Hsp33. *Mol Cell* **17:**381-392.
20. **Müller A, Langklotz S, Lupilova N, Kuhlmann K, Bandow JE, Leichert LIO.** 2014. Activation of RidA chaperone function by N-chlorination. *Nat Comm* **5:**5804.
21. **Voth W, Jakob U.** 2017. Stress-Activated Chaperones: A First Line of Defense. *Trends Biochem. Sci.* **42:**899-913.
22. 2019. Global tuberculosis report 2019. World Health Organization, Geneva.
23. **Becker SH, Jastrab JB, Dhabaria A, Chaton CT, Rush JS, Korotkov KV, Ueberheide B, Darwin KH.** 2019. The *Mycobacterium tuberculosis* Pup-proteasome system regulates nitrate metabolism through an essential protein quality control pathway. *Proc Natl Acad Sci U S A* **116:**3202-3210.
24. **Stewart GR, Wernisch L, Stabler R, Mangan JA, Hinds J, Laing KG, Young DB, Butcher PD.** 2002. Dissection of the heat-shock response in Mycobacterium tuberculosis using mutants and microarrays. *Microbiology* **148:**3129-3138.
25. **Sharp JD, Singh AK, Park ST, Lyubetskaya A, Peterson MW, Gomes AL, Potluri LP, Raman S, Galagan JE, Husson RN.** 2016. Comprehensive Definition of the SigH Regulon of *Mycobacterium tuberculosis* Reveals Transcriptional Control of Diverse Stress Responses. *PLoS One* **11:**e0152145.
26. **Vaubourgeix J, Lin G, Dhar N, Chenouard N, Jiang X, Botella H, Lupoli T, Mariani O, Yang G, Ouerfelli O, Unser M, Schnappinger D, McKinney J, Nathan C.** 2015. Stressed mycobacteria use the chaperone ClpB to sequester irreversibly oxidized proteins asymmetrically within and between cells. *Cell Host Microbe* **17:**178-190.
27. **Stewart GR, Newton SM, Wilkinson KA, Humphreys IR, Murphy HN, Robertson BD, Wilkinson RJ, Young DB.** 2005. The stress-responsive chaperone alpha-crystallin 2 is required for pathogenesis of *Mycobacterium tuberculosis. Mol Microbiol* **55:**1127-1137.
28. **Stewart GR, Snewin VA, Walzl G, Hussell T, Tormay P, O'Gaora P, Goyal M, Betts J, Brown IN, Young DB.** 2001. Overexpression of heat-shock proteins reduces survival of *Mycobacterium tuberculosis* in the chronic phase of infection. *Nat Med* **7:**732-737.

29. **Kapopoulou A, Lew JM, Cole ST.** 2011. The MycoBrowser portal: a comprehensive and manually annotated resource for mycobacterial genomes. *Tuberculosis* **91:**8-13.
30. **Kelley LA, Mezulis S, Yates CM, Wass MN, Sternberg MJE.** 2015. The Phyre2 web portal for protein modeling, prediction and analysis. *Nat Protocols* **10:**845.
31. **Krishna SS, Majumdar I, Grishin NV.** 2003. Structural classification of zinc fingers: SURVEY AND SUMMARY. *Nucleic Acids Res* **31:**532-550.
32. **Jakob U, Eser M, Bardwell JCA.** 2000. Redox Switch of Hsp33 Has a Novel Zinc-binding Motif. *J Biol Chem* **275:**38302-38310.
33. **Park OK, Bauerle R.** 1999. Metal-catalyzed oxidation of phenylalanine-sensitive 3-deoxy-D-arabino-heptulosonate-7-phosphate synthase from Escherichia coli: inactivation and destabilization by oxidation of active-site cysteines. *J Bacteriol* **181:**1636-1642.
34. **Pollard FH, Hanson P, Geary WJ.** 1959. 4-(2-Pyridylazo)-resorcinol as a possible analytical reagent for the colorimetric estimation of cobalt, lead, and uranium. *Anal Chimica Acta* **20:**26-31.
35. **Kelly SM, Jess TJ, Price NC.** 2005. How to study proteins by circular dichroism. *Biochimica et Biophysica Acta - Proteins and Proteomics* **1751:**119-139.
36. **Greenfield NJ.** 2006. Using circular dichroism spectra to estimate protein secondary structure. *Nat Protocols* **1:**2876-2890.
37. **Oh HJ, Chen X, Subjeck JR.** 1997. hsp110 Protects Heat-denatured Proteins and Confers Cellular Thermoresistance. *J Biol Chem* **272:**31636-31640.
38. **Buchner J, Grallert H, Jakob U.** 1998. Analysis of chaperone function using citrate synthase as nonnative substrate protein. *Methods Enzymol* **290:**323-338.
39. **Groitl B, Horowitz S, Makepeace KAT, Petrotchenko EV, Borchers CH, Reichmann D, Bardwell JCA, Jakob U.** 2016. Protein unfolding as a switch from self-recognition to high-affinity client binding. *Nat Comm* **7:**10357.
40. **Reichmann D, Xu Y, Cremers Claudia M, Ilbert M, Mittelman R, Fitzgerald Michael C, Jakob U.** 2012. Order out of Disorder: Working Cycle of an Intrinsically Unfolded Chaperone. *Cell* **148:**947-957.
41. **Mogk A, Deuerling E, Vorderwülbecke S, Vierling E, Bukau B.** 2003. Small heat shock proteins, ClpB and the DnaK system form a functional triade in reversing protein aggregation. *Mol Microbiol* **50:**585-595.
42. **Nathan C, Shiloh MU.** 2000. Reactive oxygen and nitrogen intermediates in the relationship between mammalian hosts and microbial pathogens. *Proc Natl Acad Sci U S A* **97:**8841-8848.
43. **Jackson SH, Gallin JI, Holland SM.** 1995. The p47phox mouse knock-out model of chronic granulomatous disease. *J Exp Med* **182:**751.
44. **Pollock JD, Williams DA, Gifford MAC, Li LL, Du X, Fisherman J, Orkin SH, Doerschuk CM, Dinauer MC.** 1995. Mouse model of X–linked chronic granulomatous disease, an inherited defect in phagocyte superoxide production. *Nat Genetics* **9:**202-209.
45. **MacMicking JD, North RJ, LaCourse R, Mudgett JS, Shah SK, Nathan CF.** 1997. Identification of nitric oxide synthase as a protective locus against tuberculosis. *Proc Natl Acad Sci U S A* **94:**5243-5248.

46. **Aratani Y, Koyama H, Nyui S-i, Suzuki K, Kura F, Maeda N.** 1999. Severe Impairment in Early Host Defense against *Candida albicans* in Mice Deficient in Myeloperoxidase. I*nfect Immun* **67:**1828.
47. **Deffert C, Cachat J, Krause K-H.** 2014. Phagocyte NADPH oxidase, chronic granulomatous disease and mycobacterial infections. *Cell Microbiol* **16:**1168-1178.
48. **Shimada H, Yamaoka Y, Morita R, Mizuno T, Gotoh K, Higuchi T, Shiraishi T, Imamura Y.** 2012. Possible mechanism of superoxide formation through redox cycling of plumbagin in pig heart. *Toxicol in Vitro* **26:**252-257.
49. **Stuehr DJ, Nathan CF.** 1989. Nitric oxide. A macrophage product responsible for cytostasis and respiratory inhibition in tumor target cells. *J Exp Med* **169:**1543-1555.
50. **Lu J, Holmgren A.** 2014. The thioredoxin antioxidant system. *Free Radical Biology and Medicine* **66:**75-87.
51. **Sassetti CM, Rubin EJ.** 2003. Genetic requirements for mycobacterial survival during infection. *Proc Natl Acad Sci U S A* **100:**12989.
52. **Abomoelak B, Marcus SA, Ward SK, Karakousis PC, Steinberg H, Talaat AM.** 2011. Characterization of a novel heat shock protein (Hsp22.5) involved in the pathogenesis of *Mycobacterium tuberculosis. J Bacteriol* **193:**3497-3505.
53. **Szklarczyk D, Gable AL, Lyon D, Junge A, Wyder S, Huerta-Cepas J, Simonovic M, Doncheva NT, Morris JH, Bork P, Jensen LJ, Mering Christian v.** 2018. STRING v11: protein–protein association networks with increased coverage, supporting functional discovery in genome-wide experimental datasets. *Nuc Acids Res* **47:**D607-D613.
54. **Zhang H, Yang J, Wu S, Gong W, Chen C, Perrett S.** 2016. Glutathionylation of the Bacterial Hsp70 Chaperone DnaK Provides a Link between Oxidative Stress and the Heat Shock Response. *J Biol Chem* **291:**6967-6981.
55. **Ho SN, Hunt HD, Horton RM, Pullen JK, Pease LR.** 1989. Site-directed mutagenesis by overlap extension using the polymerase chain reaction. Gene **77:**51-59.
56. **Hatfull GF, Jacobs WR.** 2000. Molecular Genetics of Mycobacteria. ASM Press, Washington, D.C.
57. **Samanovic MI, Tu S, Novak O, Iyer LM, McAllister FE, Aravind L, Gygi SP, Hubbard SR, Strnad M, Darwin KH.** 2015. Proteasomal control of cytokinin synthesis protects Mycobacterium tuberculosis against nitric oxide. *Mol Cell* **57:**984-994.
58. **Winter J, Ilbert M, Graf PCF, Ozcelik D, Jakob U.** 2008. Bleach activates a redox-regulated chaperone by oxidative protein unfolding. *Cell* **135:**691-701.
59. **Hunt JB, Neece SH, Ginsburg A.** 1985. The use of 4-(2-pyridylazo)resorcinol in studies of zinc release from *Escherichia coli* aspartate transcarbamoylase. *Anal Biochem* **146:**150-157.
60. **Kurganov BI.** 2002. Kinetics of Protein Aggregation. Quantitative Estimation of the Chaperone-Like Activity in Test-Systems Based on Suppression of Protein Aggregation. *Biochemistry* **67:**409-422.

61. **Pellaud J, Schote U, Arvinte T, Seelig J.** 1999. Conformation and Self-association of Human Recombinant Transforming Growth Factor-β3 in Aqueous Solutions. *J Biol Chem* **274:**7699-7704.
62. **Jastrab JB, Wang T, Murphy JP, Bai L, Hu K, Merkx R, Huang J, Chatterjee C, Ovaa H, Gygi SP, Li H, Darwin KH.** 2015. An adenosine triphosphate-independent proteasome activator contributes to the virulence of Mycobacterium tuberculosis. *Proc Natl Acad Sci U S A* **112:**E1763-1772.
63. **Lignitto L, LeBoeuf SE, Homer H, Jiang S, Askenazi M, Karakousi TR, Pass HI, Bhutkar AJ, Tsirigos A, Ueberheide B, Sayin VI, Papagiannakopoulos T, Pagano M.** 2019. Nrf2 Activation Promotes Lung Cancer Metastasis by Inhibiting the Degradation of Bach1. *Cell* **178:**316-329.e318.
64. **Choi H, Larsen B, Lin Z-Y, Breitkreutz A, Mellacheruvu D, Fermin D, Qin ZS, Tyers M, Gingras A-C, Nesvizhskii AI.** 2011. SAINT: probabilistic scoring of affinity purification–mass spectrometry data. *Nat Methods* **8:**70-73.
65. **Schäffer AA, Aravind L, Madden TL, Shavirin S, Spouge JL, Wolf YI, Koonin EV, Altschul SF.** 2001. Improving the accuracy of PSI-BLAST protein database searches with composition-based statistics and other refinements. *Nuc Acids Res* **29:**2994-3005.
66. **Tatusova T, DiCuccio M, Badretdin A, Chetvernin V, Nawrocki EP, Zaslavsky L, Lomsadze A, Pruitt KD, Borodovsky M, Ostell J.** 2016. NCBI prokaryotic genome annotation pipeline. *Nuc Acids Res* **44:**6614-6624.
67. **Shell SS, Wang J, Lapierre P, Mir M, Chase MR, Pyle MM, Gawande R, Ahmad R, Sarracino DA, Ioerger TR, Fortune SM, Derbyshire KM, Wade JT, Gray TA.** 2015. Leaderless Transcripts and Small Proteins Are Common Features of the Mycobacterial Translational Landscape. *PLoS Genet* **11:**e1005641.
68. **Chong YH, Jung JM, Choi W, Park CW, Choi KS, Suh YH.** 1994. Bacterial expression, purification of full length and carboxyl terminal fragment of Alzheimer amyloid precursor protein and their proteolytic processing by thrombin. *Life Sci* **54:**1259-1268.
69. **Darwin AJ, Miller VL.** 2001. The psp locus of Yersinia enterocolitica is required for virulence and for growth in vitro when the Ysc type III secretion system is produced. *Mol Microbiol* **39:**429-444.
70. **Garbe TR, Barathi J, Barnini S, Zhang Y, Abou-Zeid C, Tang D, Mukherjee R, Young DB.** 1994. Transformation of mycobacterial species using hygromycin resistance as selectable marker. *Microbiology* **140:**133-138.
71. **Stover CK, de la Cruz VF, Fuerst TR, Burlein JE, Benson LA, Bennett LT, Bansal GP, Young JF, Lee MH, Hatfull GF, et al.** 1991. New use of BCG for recombinant vaccines. *Nature* **351:**456-460.